

AD-757 526

NEAR FIELD SMALL EARTHQUAKES - DIS-
LOCATION MOTION

Yi-Ben Tsai, et al

Texas Instruments, Incorporated

Prepared for:

Air Force Office of Scientific Research

15 November 1972

DISTRIBUTED BY:

NTIS

**National Technical Information Service
U. S. DEPARTMENT OF COMMERCE
5285 Port Royal Road, Springfield Va. 22151**

**BEST
AVAILABLE COPY**



NEAR FIELD SMALL EARTHQUAKES - DISLOCATION MOTION

Semi-Annual Technical Report No. 1
1 May 1972 to 31 October 1972

Prepared by
Yi-Ben Tsai and Howard J. Patton

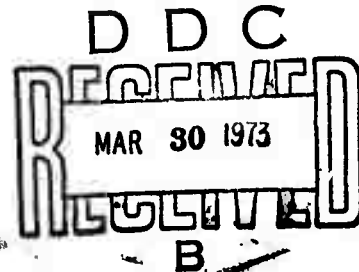
Yi-Ben Tsai, Project Scientist
Area Code 703, 836-3882 Ext. 305

T. W. Harley, Program Manager
Area Code 703, 836-3882 Ext. 300

TEXAS INSTRUMENTS INCORPORATED

Services Group
Post Office Box 5621
Dallas, Texas 75222

Contract No. F44620-72-C-0073
Amount of Contract: \$51,164
Beginning 1 May 1972
Ending 30 April 1973



Prepared for

AIR FORCE OFFICE OF SCIENTIFIC RESEARCH

Sponsored by

ADVANCED RESEARCH PROJECTS AGENCY
Nuclear Monitoring Research Office
ARPA Order No. 2134
ARPA Program Code No. 2F10

Reproduced by
**NATIONAL TECHNICAL
INFORMATION SERVICE**
U S Department of Commerce
Springfield VA 22151

15 November 1972

Acknowledgement: This research was supported by the Advanced Research Projects Agency, Nuclear Monitoring Research Office, under Project VELA-UNIFORM, and accomplished under the direction of the Air Force Office of Scientific Research under Contract No. F44620-72-C-0073.

**Approved for public release;
distribution unlimited.**

AD 757526

DOCUMENT CONTROL DATA - R & D

(Security classification of title, body of abstract and indexing annotation must be entered when the overall report is classified)

1. ORIGINATING ACTIVITY (Corporate author) Texas Instruments Incorporated Services Group P.O. Box 5621, Dallas, Texas 75222		2a. REPORT SECURITY CLASSIFICATION UNCLASSIFIED	
		2b. GROUP	
3. REPORT TITLE Near Field Small Earthquakes - Dislocation Motion, Semi-Annual Technical Report No. 1			
4. DESCRIPTIVE NOTES (Type of report and inclusive dates) Scientific - Interim			
5. AUTHOR(S) (First name, middle initial, last name) Yi-Ben Tsai and Howard J. Patton			
6. REPORT DATE 15 November 1972	7a. TOTAL NO. OF PAGES 6162	7b. NO. OF REFS 8	
8a. CONTRACT OR GRANT NO. F44620-72-C-0073	8b. PROJECT NO. AO 2134		
c. 62701D	9a. ORIGINATOR'S REPORT NUMBER(S)		
	9b. OTHER REPORT NO(S) (Any other numbers that may be assigned this report) AFOSR - TR - 73 - 0496		
10. DISTRIBUTION STATEMENT Approved for public release; Distribution unlimited.			
11. SUPPLEMENTARY NOTES TECH, OTHER		12. SPONSORING MILITARY ACTIVITY Air Force Office of Scientific Research/NP 1400 Wilson Boulevard Arlington, VA 22209	
13. ABSTRACT Fifty-one three-component strong motion records have been digitized in a unified file on magnetic tape for rapid processing of observed accelerograms. Computer programs have been developed to calculate theoretical velocity waveforms by differentiating displacement waveforms computed according to Haskell's dislocation model and to calculate experimental waveforms by integration of the digitized acceleration records. An evaluation of methods to obtain experimental waveforms has revealed that velocity waveforms are far less sensitive to various schemes of numerical integration and base-lines corrections than displacement waveforms; therefore, comparison of experimental and theoretical waveforms will be carried out at the velocity level. Linear and cubic least squares corrections of the accelerogram and the integrated velocity waveform respectively have been found to result in reasonably reliable experimental velocity waveforms for interpretation with a moving dislocation model. A theoretical velocity waveform based on a linear ramp dislocation source time function appears to be superior to one based on an exponential ramp function when compared with the experimental waveform to interpret observed records. Dislocation processes associated with Parkfield and San Fernando earthquakes have been determined using the moving dislocation model.			



NEAR FIELD SMALL EARTHQUAKES - DISLOCATION MOTION

Semi-Annual Technical Report No. 1
1 May 1972 to 31 October 1972

Prepared by
Yi-Ben Tsai and Howard J. Patton

Yi-Ben Tsai, Project Scientist
Area Code 703, 836-3882 Ext. 305

T. W. Harley, Program Manager
Area Code 703, 836-3882 Ext. 300

TEXAS INSTRUMENTS INCORPORATED
Services Group
Post Office Box 5621
Dallas, Texas 75222

Contract No. F44620-72-C-0073
Amount of Contract: \$51,164
Beginning 1 May 1972
Ending 30 April 1973

Prepared for
AIR FORCE OFFICE OF SCIENTIFIC RESEARCH

Sponsored by
ADVANCED RESEARCH PROJECTS AGENCY
Nuclear Monitoring Research Office
ARPA Order No. 2134
ARPA Program Code No. 2F10

15 November 1972

Acknowledgement: This research was supported by the Advanced Research Projects Agency, Nuclear Monitoring Research Office, under Project VELA-UNIFORM, and accomplished under the direction of the Air Force Office of Scientific Research under Contract No. F44620-72-C-0073.

Approved for public release;
distribution unlimited.

TABLE OF CONTENTS

SECTION	TITLE	PAGE
I.	INTRODUCTION	I-1
II.	ORGANIZATION OF THE DATA BASE	II-1
III.	DATA PROCESSING PROCEDURES	III-1
IV.	AN EVALUATION OF VELOCITY AND DISPLACEMENT TRACES IN COMPARI- SONS BETWEEN ACCELEROGRAM DATA AND THE SOURCE MODEL	IV-1
V.	INTERPRETATION OF THE EARTH- QUAKE STRONG-MOTION RECORDS BY A MOVING DISLOCATION MODEL	V-1
	A. THE SAN FERNANDO EARTH- QUAKE OF FEBRUARY 9, 1971	V-4
	B. THE PARKFIELD EARTHQUAKE OF JUNE 28, 1966	V-10
VI.	EVALUATION OF TWO DISLOCATION TIME FACTORS	VI-1
VII.	SUMMARY	VII-1
VIII.	REFERENCES	VIII-1

LIST OF FIGURES

FIGURE	TITLE	PAGE
II-1	DATA FILE FORMAT	II-2
II-2	DATA FILE HEADER CONTENTS	II-3
II-3	CARD ERROR CHECK PRINTOUT	II-4
II-4	CARD TO TAPE MONITOR PRINTOUT	II-6
II-5	TAPE TO TAPE MONITOR PRINTOUT	II-7
III-1	RESULTANT VELOCITY AND DISPLACEMENT WAVEFORMS FROM A TRAPEZOIDAL (LINEAR) INTEGRATION SCHEME	III-2
III-2	RESULTANT VELOCITY AND DISPLACEMENT WAVEFORMS FROM A QUADRATIC INTER- POLATION AND INTEGRATION BY LEGENDRE- GAUSSIAN QUADRATURE	III-3
III-3	ACCELEROGRAM RECORD, N65°E COMPONENT, PARKFIELD EARTHQUAKE, JUNE 27, 1966, CHOLAME, CAL., ST. #2	III-6
III-4	RESULTANT VELOCITY AND DISPLACEMENT WAVEFORMS FROM AN ACCELEROGRAM (SAME RECORD IN FIG. III-1) WITHOUT A BASELINE FIT	III-7
III-5	RESULTANT VELOCITY AND DISPLACEMENT WAVEFORMS FROM AN ACCELEROGRAM WITH A BASELINE FIT	III-8
III-6	UNCORRECTED VELOCITY TRACE (FITTED CORRECTION CUBIC SHOWN WITH IT) AND RESULTANT DISPLACEMENT TRACE	III-11
III-7	CORRECTED VELOCITY TRACE (INTERVAL OF FIT [0, 10]) AND RESULTANT DIS- PLACEMENT TRACE	III-12
III-8	FUNCTIONAL CHARACTERISTICS OF THE CORRECTION CUBIC	III-13

LIST OF FIGURES
(continued)

FIGURE	TITLE	PAGE
IV-1	CORRECTED VELOCITY TRACE (INTERVAL OF FIT [0, 44]) AND RESULTANT DISPLACEMENT TRACE	IV-2
IV-2	CORRECTED VELOCITY TRACE USING NON-FITTED CUBIC BUT CONSTRAINED TO INTERSECT THE UNCORRECTED VELOCITY TRACE AT 0, 15, 21, 30 SECONDS AND RESULTANT DISPLACEMENT TRACE. S74°W ACCELEROGRAM COMPONENT, SAN FERNANDO EARTHQUAKE FEB. 9, 1971, PACOIMA DAM SITE	IV-3
IV-3	CORRECTED VELOCITY TRACE USING NON-FITTED CUBIC BUT CONSTRAINED TO INTERSECT UNCORRECTED VELOCITY TRACE AT 0, 16, 22, 30 SECONDS AND THE RESULTANT DISPLACEMENT TRACE	IV-5
V-1	THE COORDINATE SYSTEM AND THE FAULT PLANE GEOMETRY	V-2
V-2	THE ACCELERATION WAVEFORMS DUE TO THE SAN FERNANDO EARTHQUAKE OF FEB. 9, 1971 RECORDED AT THE PACOIMA DAM ACCELEROGRAPH SITE	V-5
V-3	THE OBSERVED (IN SOLID CURVES) AND THE THEORETICAL (IN DASHED CURVES) VELOCITY WAVEFORMS OF THE SAN FERNANDO EARTHQUAKE AS SEEN AT THE PACOIMA DAM SITE	V-6
V-4	THE HORIZONTAL PROJECTION OF THE ASSUMED FAULT PLANE AS COMPARED WITH THE LOCATIONS OF THE PACOIMA DAM ACCELEROGRAPH, THE SAN FERNANDO EARTHQUAKE AND ITS AFTERSHOCKS	V-8
V-5	THE THEORETICAL VELOCITY WAVEFORMS AT THE PACOIMA DAM SITE IF THE STRIKE-SLIP DISLOCATION COMPONENT AMOUNTS TO ONE HALF OF THE THRUST DISLOCATION	V-9

LIST OF FIGURES
(continued)

FIGURE	TITLE	PAGE
V-6	THE LOCATION OF STATION 2 ACCELEROGRAPH WITH RESPECT TO THE SAN ANDREAS FAULT TRACE AND THE SURFACE CRACKS DUE TO THE PARKFIELD EARTHQUAKE OF JUNE 28, 1966	V-12
V-7	A. THE OBSERVED HORIZONTAL ACCELERATION WAVEFORM IN THE N65°E COMPONENT AT STATION 2 DURING THE PARKFIELD EARTHQUAKE OF JUNE 28, 1966; B. THE CORRESPONDING OBSERVED (SOLID CURVE) AND THEORETICAL (DASHED CURVE) VELOCITY WAVEFORMS	V-13
V-8	THE THEORETICAL VELOCITY WAVEFORM FOR A MOVING STRIKE-SLIP DISLOCATION WITH $W = 3.0$ KM, $L = 6.4$ KM, $V = 2.2$ KM/SEC, $T = 0.8$ SEC, $D_0 = 200$ CM	V-15
V-9	THE THEORETICAL VELOCITY WAVEFORM FOR A MOVING STRIKE-SLIP DISLOCATION WITH $W = 3.0$ KM, $L = 6.4$ KM, $V = 2.2$ KM/SEC, $T = 0.4$ SEC, $D_0 = 200$ CM	V-16
VI-1	LINEAR AND EXPONENTIAL RAMP DISLOCATION TIME FUNCTIONS AND THEIR ASSOCIATED VELOCITY FUNCTIONS	VI-2
VI-2	THEORETICAL VELOCITY WAVEFORMS, LINEAR RAMP FUNCTION WITH RISE TIME = 0.6 SECONDS	VI-3
VI-3	THEORETICAL VELOCITY WAVEFORMS, EXPONENTIAL RAMP FUNCTION WITH RISE TIME = 0.3 SECONDS	VI-4
VI-4	THEORETICAL VELOCITY WAVEFORMS, EXPONENTIAL RAMP FUNCTION WITH RISE TIME = 0.6 SECONDS	VI-5

SECTION I INTRODUCTION

A study to apply the moving dislocation model for interpretation of near-field earthquake strong-motion records has been in progress for six months. This semi-annual report gives an account of what has been accomplished to date.

Digitized raw strong-motion accelerograms were acquired directly from the Earthquake Engineering Research Laboratory of the California Institute of Technology or through the National Geophysical Data Center of NOAA. These raw data have been checked and reorganized into a uniform format and stored on a magnetic tape for processing and analysis. Section II describes in detail the reorganization of this data base.

Our analysis relies heavily on comparing the observed and the theoretically computed waveforms. Since the observed waveforms are given at the acceleration level whereas the theoretical waveforms are initially obtained at the displacement level, processing of either or both of these two waveforms is required before comparison analysis can be undertaken. Problems are more likely to come from the observed waveforms which contain many more features than a highly idealized model can explain. Thus, Section III is devoted to an evaluation of data processing procedures which are followed in order to obtain integrated velocity and displacement waveforms from the recorded accelerograms. This discussion is followed by an evaluation of the integrated velocity and displacement waveforms (Section IV) to determine which type is more suitable for comparison with their theoretical counterparts.

In Section V preliminary results from analysis of the Pacoima Dam site accelerograms during the San Fernando earthquake of February 9, 1971 and the Station 2 accelerograms during the Parkfield earthquake of June 28, 1966 are presented. In Section VI the theoretical velocity waveforms based on linear and exponential ramp dislocation time functions are compared with the integrated experimental waveforms to determine which one of these two source time functions explains the observations better. Finally, Section VII gives a summary of the work accomplished to date.

SECTION II

ORGANIZATION OF THE DATA BASE

To insure ease of future handling, the raw data that was acquired for this project was stored in a standard format on nine-track magnetic tape. Since the raw data was received on cards and on magnetic tape, the software for organizing it incorporated capabilities to handle both input types and their respective formats.

Primary importance was placed on designing the software to standardize the storage data file. Figure II-1 shows the format of each data file; this file format was chosen to save storage space and to conform as closely as possible to the input formats. The acquired data consists of 52 digitized three-component strong-motion accelerogram records sent from the California Institute of Technology and NOAA. Consequently, the data file is broken down into a header record and three data records. The header record is also standardized and contains sufficient information to identify the accelerogram record and to read the data records from tape. An example of a header record is given in Figure II-2.

Thirty six accelerogram records were received on cards. Before these records were stored on tape, a thorough check for errors was required. Preliminary processing had uncovered errors such as duplicate cards and invalid characters. Therefore, software was written to search the cards for errors of this nature. Figure II-3 is a sample of the output from this processing. The cards were corrected using references which listed valid data.

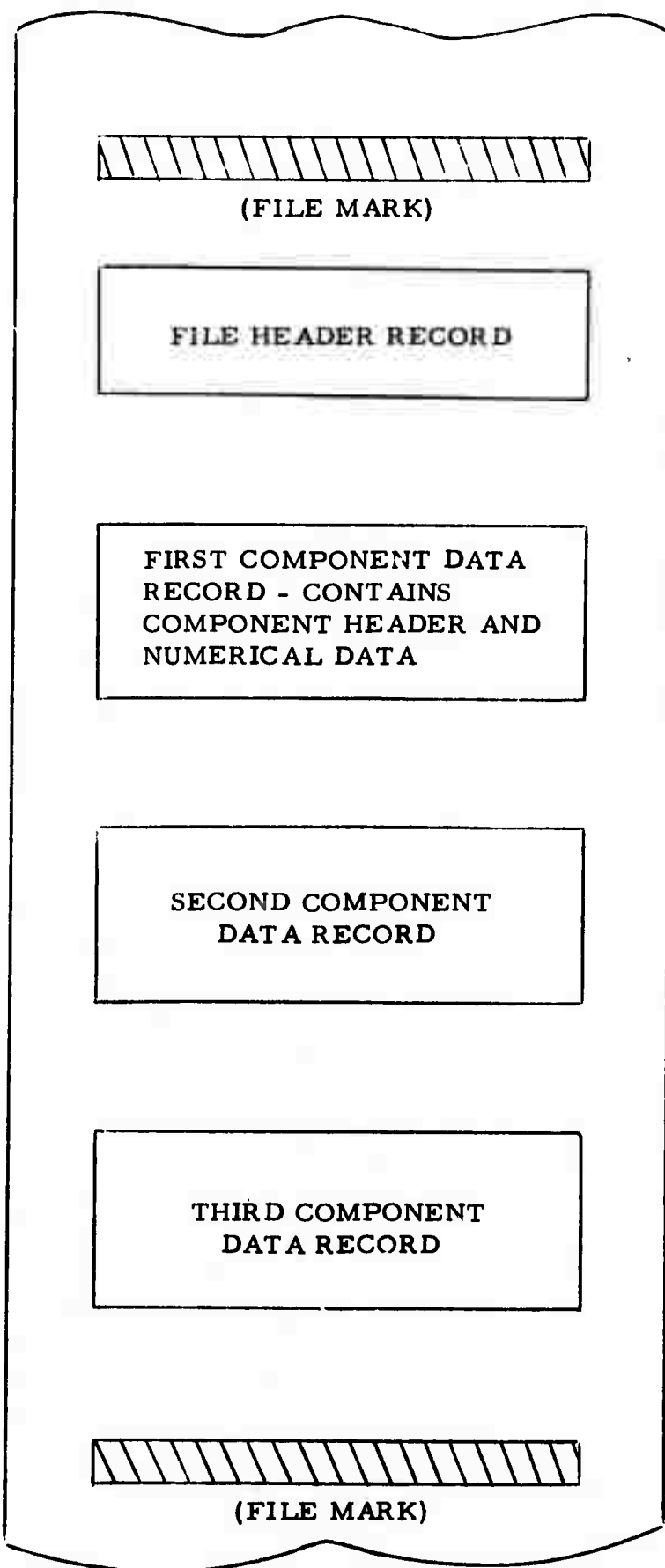


FIGURE II-1
DATA FILE FORMAT

TIHEADER
TAPE NO. L16294
FILE NO. 5
RECORD NO. IA5
NO. OF COMPONENTS 3
LENGTHS OF COMPONENT HEADERS(IN BYTES) 240 , 240 , 240
NO. OF DATA POINTS FOR EACH COMPONENT(IN BYTES) 7056 , 7760 , 9888

OPEN FILE CODE=C00000000

FIGURE II-2
DATA FILE HEADER CONTENTS

02 51.1T FERNDALÉ CAL OCT 7 1951 S44W

SCALED DATA, FIXED TRACE, TIMING MARKS, ALIGNMENT CORRECTIONS.

UNITS ARE SEC, G/10.

021
021
021

COMPONENT
HEADER

02 51.1T FERNDALÉ CAL OCT 7 1951 N46W

SCALED DATA, FIXED TRACE, TIMING MARKS, ALIGNMENT CORRECTIONS.

UNITS ARE SEC, G/10.

022
022
022
022 68
022134
022144

17.168 -0.103 17.241 *0.062 17.308 0.C**17.386 -0.032 1*.481 0.030
*7.780 -0.016 48.002 0.00..48.175 0.C01 48..17 0.001 48...8 -0.011
55.480 -0.015 55.678 0.008 55.766 0.030 55.873 0.006 0.0 *****

CARDS HAVING
INVALID CHARACTERS
ARE PRINTED OUT

02 51.1T FERNDALÉ CAL OCT 7 1951 VERT

SCALED DATA, FIXED TRACE, TIMING MARKS, ALIGNMENT CORRECTIONS.

UNITS ARE SEC, G/10.

023
023
023

FIGURE II-3
CARD ERROR CHECK PRINTOUT

Having completed the error scal process, the data on cards was ready for storage. Information for each file header was punched on cards. On-line checks between file header information and component header information prevented any disordering of data. An example of the printed output, shown in Figure II-4, illustrates how the process was monitored.

The remaining 15 accelerogram records were received on seven-track magnetic tape. The contents of this tape were stored alphanumerically in a card image format. Hence, the software for this tape-to-tape process was designed to convert the input data to a floating point representation and then store it on nine-track tape in standardized files. Error monitoring and correction was accomplished during data conversion. Information for the file header was extracted from the component headers during the processing. The printed output for the tape-to-tape operations, an example of which is shown in Figure II-5, provided a means of monitoring the processing.

OUTFILE 35

TIHFADERTAPE NO. L16294 FILE NO.35 RFCORD NO. 1839 NO. OF COMPONENTS 3
LENGTHS OF COMPONENT HEADERS(IN BYTES) 240 240 240 NO. OF DATA POINTS FOR EACH
COMPONENT(IN BYTES) 2848 2768 2616
WRITE ERROR CODE=00000000

1ST COMPONENT NO. OF BYTES WRITTEN= 3088 WRITE ERROR CODE=00000000
2ND COMPONENT NO. OF BYTES WRITTEN= 3008 WRITE ERROR CODE=00000000
3RD COMPONENT NO. OF BYTES WRITTEN= 2856 WRITE ERROR CODE=00000000

END OF OUTFILE 35

OUTFILE 36

TIHFADERTAPE NO. L16294 FILE NO.36 RFCORD NO. 1840 NO. OF COMPONENTS 3
LENGTHS OF COMPONENT HEADERS(IN BYTES) 240 240 240 NO. OF DATA POINTS FOR EACH
COMPONENT(IN BYTES) 5768 4792 5672
WRITE ERROR CODE=00000000

1ST COMPONENT NO. OF BYTES WRITTEN= 6008 WRITE ERROR CODE=00000000
2ND COMPONENT NO. OF BYTES WRITTEN= 5032 WRITE ERROR CODE=00000000
3RD COMPONENT NO. OF BYTES WRITTEN= 5912 WRITE ERROR CODE=00000000

END OF OUTFILE 36

FIGURE II-4

CARD TO TAPE MONITOR PRINTOUT

INFILE 16 READ ERROR CODE=0CF
COMPDATA CONVERSION COMPLETED.

INFILE 17 READ ERROR CODE=0CF
COMPDATA CONVERSION COMPLETED.

INFILE 18 READ ERROR CODE=0CF
COMPDATA CONVERSION COMPLETED.

OUTFILE 42

TITMADERTAPE NO. L16294 FILE NO.42 RECORD NO. 10046 NO. OF COMPONENTS 3
LENGTHS OF COMPONENT HEADERS(IN BYTES) 960 960 960 NO. OF DATA POINTS FOR EACH
COMPONENT(IN BYTES) 5564 8232 6888
WRITE ERROR CODE=00000000

1ST COMPONENT NO. OF BYTES WRITTEN=10564 WRITE ERROR CODE=00000000

2ND COMPONENT NO. OF BYTES WRITTEN= 9192 WRITE ERROR CODE=00000000

3RD COMPONENT NO. OF BYTES WRITTEN= 7848 WRITE ERROR CODE=00000000

END OF OUTFILE 42

FIGURE II-5

TAPE TO TAPE MONITOR PRINTOUT

SECTION III

DATA PROCESSING PROCEDURES

Digitized strong-motion accelerogram records are integrated twice to obtain ground velocity and ground displacement records. These traces are compared with results computed from a moving dislocation source model. The integration was carried out by a Legendre-Gaussian Quadrature which incorporated a quadratic interpolation scheme. Since the Legendre-Gaussian Quadrature will compute exactly the integrals for any order polynomial, the degree of accuracy depends solely on the order of the polynomial used for interpolating. Figures III-1 and III-2 show the results of two integration schemes. Figure III-1 are results from linear interpolation (trapezoidal integration), and Figure III-2 are results from quadratic interpolation. Comparison shows that the general characteristic of the integrated traces are very similar. However, the differences in values for velocity and displacement are large enough to justify the use of quadratic interpolation.

The application of baseline corrections for the accelerogram and velocity trace are crucial in improving the quality of the integrated traces. The baseline for the accelerogram is found by fitting a straight line to the accelerogram record. The linear equation obtained from this process is used for the baseline. Mathematically, this may be expressed as follows:

Let:

A_i be the raw acceleration at time, t_i ,

—1833 06.1 CHOLAME--SHANDON.CAI .ND2, JUN 27 65. 2026PST, N65E

DISPLACEMENT

1.05723

VELOCITY

1.80401

ACCELERATION

0.29475

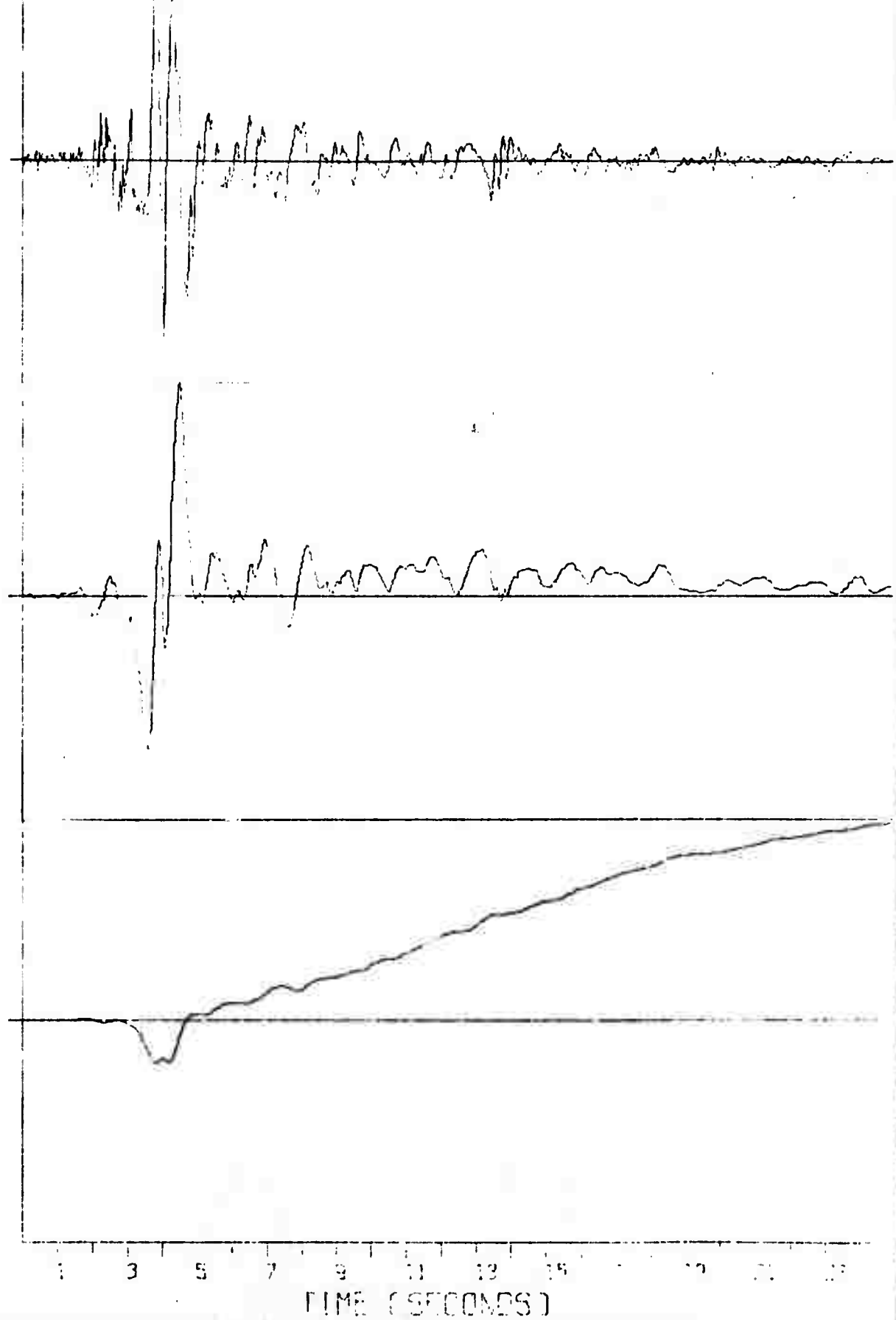


FIGURE III-1

RESULTANT VELOCITY AND DISPLACEMENT WAVEFORMS
FROM A TRAPEZOIDAL (LINEAR) INTEGRATION SCHEME

1833 06.11. PFC CLAME--SHANDON. CAL, NO2, JUN 27 65. 2026PST, NOISE

DISPLACEMENT

1.95397

VELOCITY

1.63191

ACCELERATION

0.29476

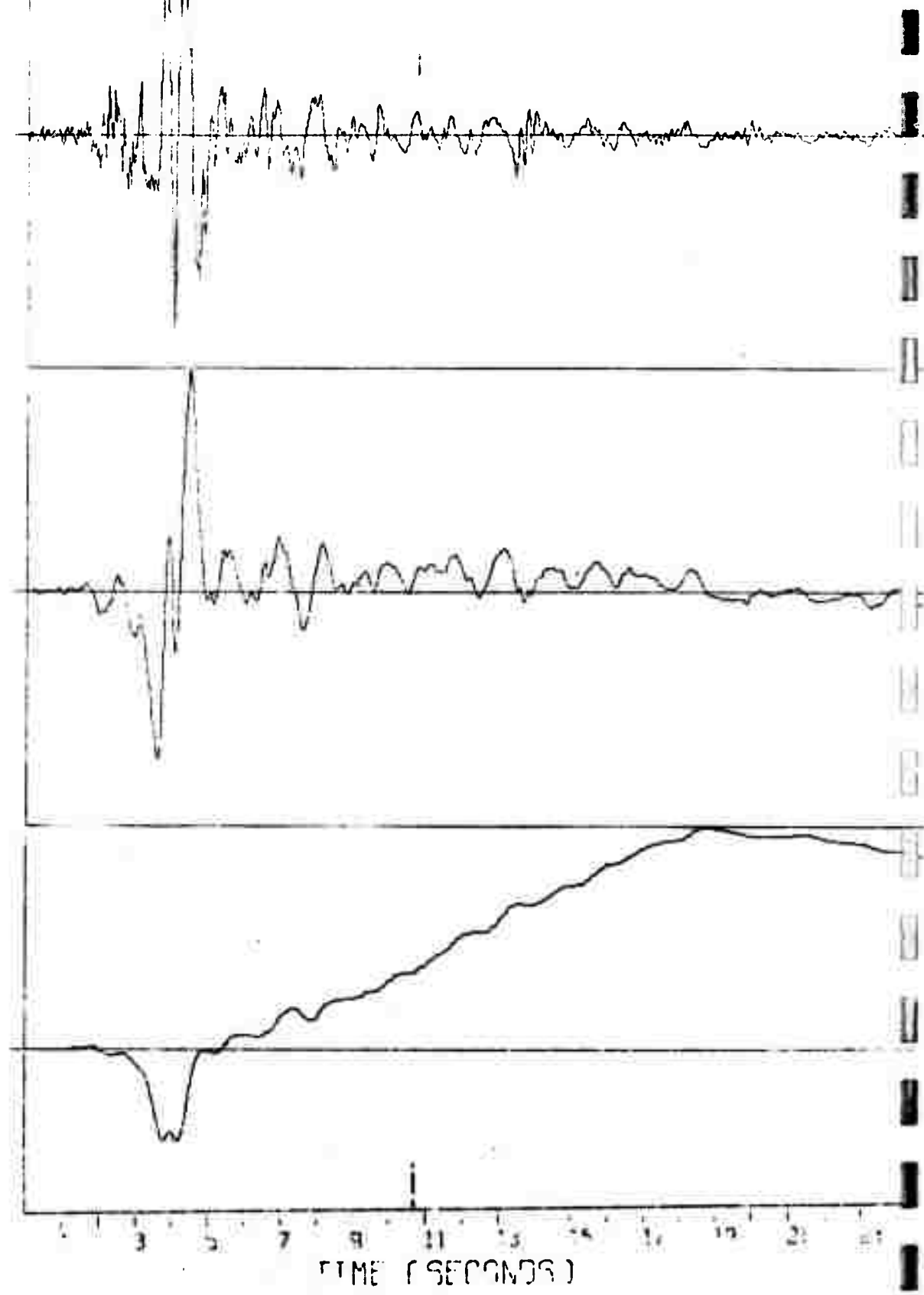


FIGURE III-2
RESULTANT VELOCITY AND DISPLACEMENT WAVEFORMS
FROM A QUADRATIC INTERPOLATION AND INTEGRATION
BY LE GENDRE-GAUSSIAN QUADRATURE

$L(t_i) = L_0 + L_1(t_i)$ be a linear equation in time, t_i , used as the baseline.

Thus, the corrected record $\Delta_{A_i}(t_i)$ is:

$$\Delta_{A_i}(t_i) = A_i - L(t_i)$$

Using the least squares criterion to estimate L_0 and L_1 requires that

$\sum_{i=a}^b \Delta_{A_i}^2(t_i)$ be a minimum over a given interval $[t_a, t_b]$.

That is:

$$\frac{\partial}{\partial L_0} \sum_{i=a}^b \Delta_{A_i}^2(t_i) = 0$$

and

$$\frac{\partial}{\partial L_1} \sum_{i=a}^b \Delta_{A_i}^2(t_i) = 0$$

Taking the partial derivatives and solving for L_0 and L_1 yields

$$L_0 = \frac{\begin{vmatrix} \sum_{i=a}^b A_i & \sum_{i=a}^b t_i \\ \sum_{i=a}^b t_i A_i & \sum_{i=a}^b t_i^2 \end{vmatrix}}{D}$$

$$L_1 = \frac{\begin{vmatrix} N & \sum_{i=a}^b A_i \\ \sum_{i=a}^b t_i & \sum_{i=a}^b t_i A_i \end{vmatrix}}{D}$$

where N = number of data points in the interval $[t_a, t_b]$.

and

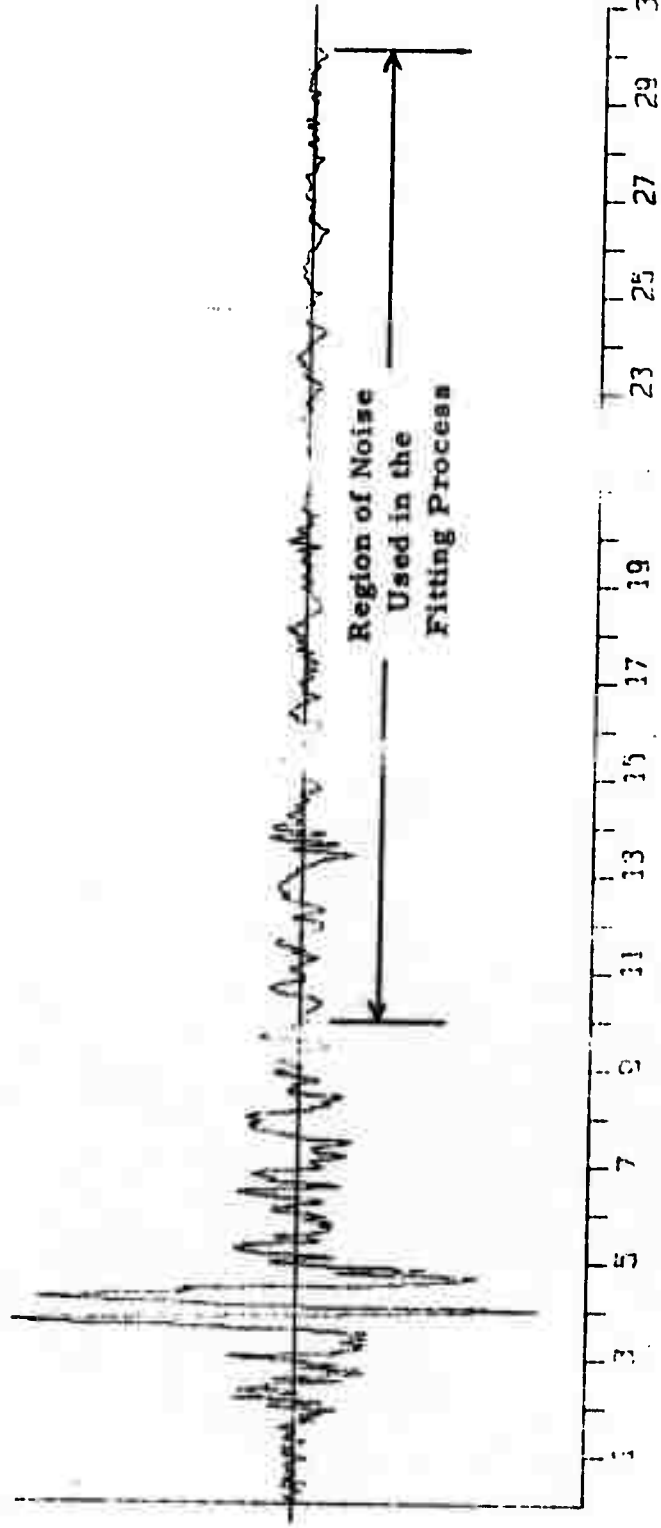
D =

$$\begin{vmatrix} N & \sum_{i=a}^b t_i \\ \sum_{i=a}^b t_i & \sum_{i=a}^b t_i^2 \end{vmatrix}$$

This fitting process may be applied to the accelerogram record over any chosen interval $[t_a, t_b]$. For example, consider the accelerogram in Figure III-3. It has been found that for this particular record (and in general) a better linear fit can be achieved in the regions of noise as indicated on the figure. Therefore, the interval $[10, 30]$ is chosen for the fit, and a baseline is obtained. New accelerations are computed for the entire record $[0, 30]$ relative to this new baseline.

The preciseness of the baseline fit does not appear to be critical to later processing; changes in the velocity and displacement traces resulting from the baseline correction method usually are small, as can be seen by comparing Figures III-4 (without baseline correction) and III-5 (with baseline correction). Thus, a linear fit for the baseline determination appears to be adequate in that it serves to eliminate slight drifting in the accelerogram record but does not significantly alter estimates of the velocity and displacement waveform.

The region containing first motions of the shock is of most interest in the comparison studies with the theoretical model. Therefore, in preparation for the velocity correction process, the trace is truncated to a length of approximately ten seconds centered about the shock, thereby constraining the correction to this region. The correction process involves a least squares fit of a cubic curve to the ten second velocity trace. This order fit was found to adequately cancel long-period noise without affecting the important characteristics of first motion pulses. The equations for this fit may be derived following an approach similar to that outlined above



0.29476

ACCELERATION

FIGURE III-3
 ACCELEROGRAM RECORD, N65°E COMPONENT,
 PARKFIELD EARTHQUAKE, JUNE 27, 1966,
 CHOLAME, CAL., ST. #2

16.11.70: PRT - CHE, DCU, OFD, NSD

VELOCITY

0.0189C

DISPLACEMENT

0.02074

0.29407

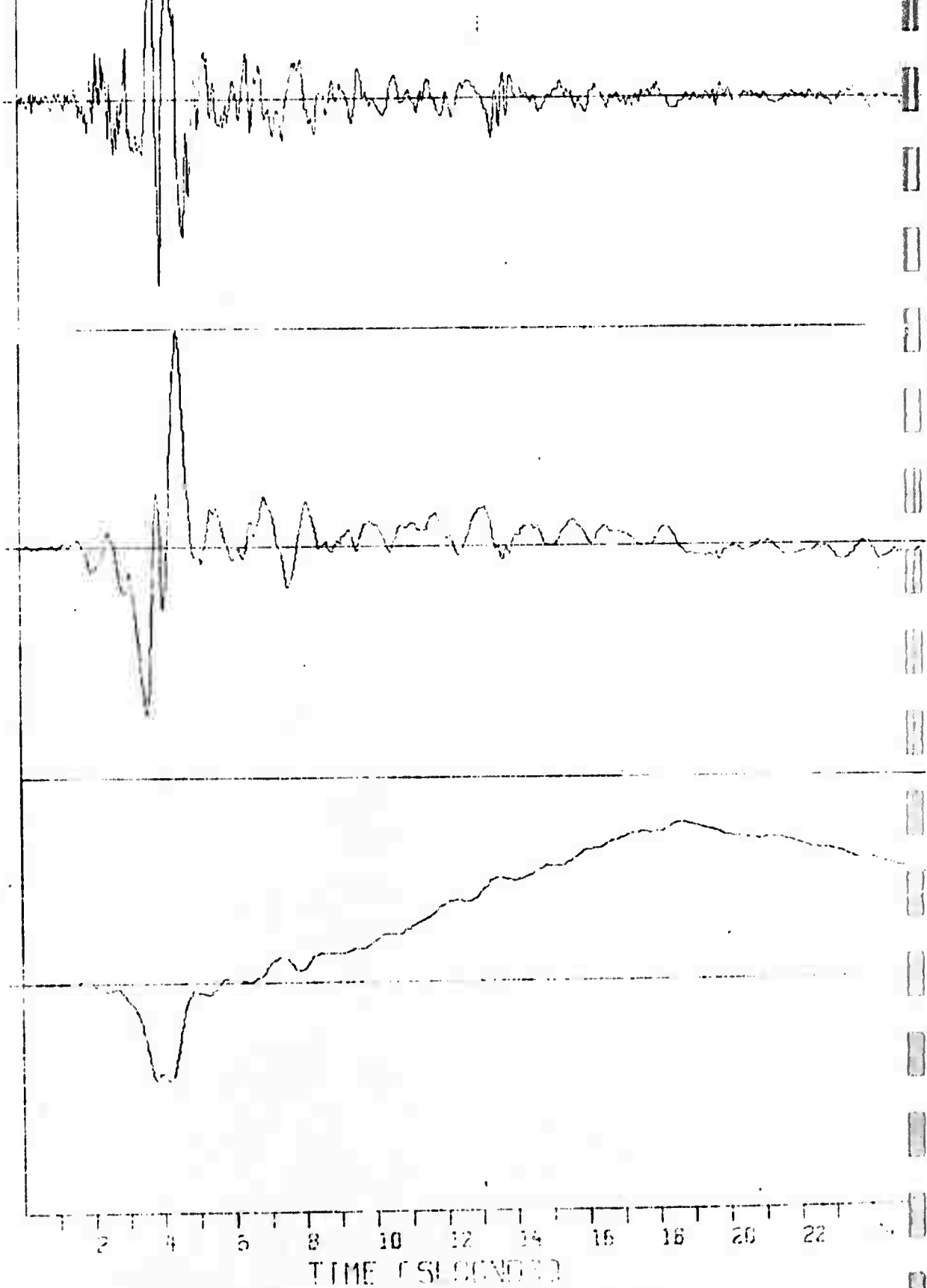


FIGURE II-4

RESULTANT VELOCITY AND DISPLACEMENT WAVEFORMS FROM AN ACCELEROGRAM WITHOUT A BASELINE FIT

1533 66. 11. CHOLAME-SHANNON. CAL. NO2. JUN 27 66. 2026PST. N65E

DISPLACEMENT

0.01994

VELOCITY

0.01869

ACCELERATION

0.29476

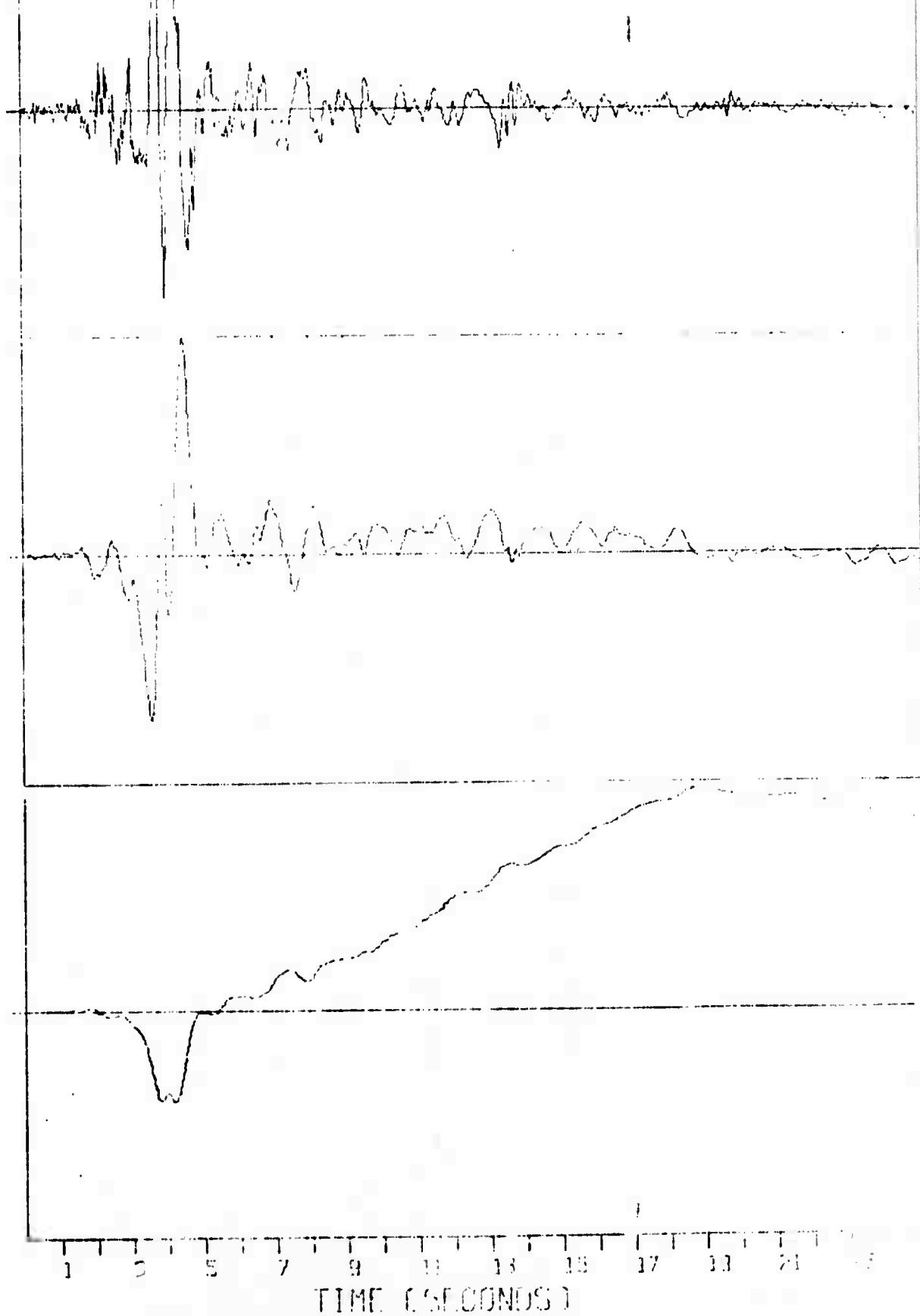


FIGURE III-5

RESULTANT VELOCITY AND DISPLACEMENT WAVEFORMS
FROM AN ACCELEROGRAM WITH A BASELINE FIT

for the linear case.

V_i = uncorrected velocity at t_i on the interval

$[t_c, t_d]$ where $t_d = t_c + 10$ sec.

$C(t_i) = C_0 + C_1 t_i + C_2 t_i^2 + C_3 t_i^3 =$ a cubic equation

in time, t_i , used for correction.

$$C_0 = 0$$

$$C_1 = \begin{vmatrix} \sum_i t_i V_i & \sum_i t_i^3 & \sum_i t_i^4 \\ \sum_i t_i^2 V_i & \sum_i t_i^4 & \sum_i t_i^5 \\ \sum_i t_i^3 V_i & \sum_i t_i^5 & \sum_i t_i^6 \end{vmatrix} / D$$

$$C_2 = \begin{vmatrix} \sum_i t_i^2 & \sum_i t_i V_i & \sum_i t_i^4 \\ \sum_i t_i^3 & \sum_i t_i^2 V_i & \sum_i t_i^5 \\ \sum_i t_i^4 & \sum_i t_i^3 V_i & \sum_i t_i^6 \end{vmatrix} / D$$

$$C_3 = \begin{vmatrix} \sum_i t_i^2 & \sum_i t_i^3 & \sum_i t_i V_i \\ \sum_i t_i^3 & \sum_i t_i^4 & \sum_i t_i^2 V_i \\ \sum_i t_i^4 & \sum_i t_i^5 & \sum_i t_i^3 V_i \end{vmatrix} / D$$

where

$$D = \begin{vmatrix} \sum_i t_i^2 & \sum_i t_i^3 & \sum_i t_i^4 \\ \sum_i t_i^3 & \sum_i t_i^4 & \sum_i t_i^5 \\ \sum_i t_i^4 & \sum_i t_i^5 & \sum_i t_i^6 \end{vmatrix}$$

and all summations run from $i = c$ to d .

The corrected velocities $\Delta_V(t_i)$ then are computed from the equation:

$$\Delta_V(t_i) = V_i - C(t_i)$$

In this analysis the cubic fit is constrained to zero at t_i in order that the initial condition for the velocity trace ($V_c = 0$) remain unchanged. The contrast between Figures III-6 and III-7 illustrates the typical effectiveness of this correction process. The dotted line through the uncorrected velocity trace in Figure III-6 is the correction cubic curve which is subtracted from that trace to obtain the velocity trace in Figure III-7. The functional characteristics of the correction cubic curve in Figure III-8 provides a quick evaluation of the fitting process.

1433 65.1T.CIVILONE-SHANNON.CAL.002.JUN 27 66.202EPT1.NOFF

DISPLACEMENT

0.00528

VELOCITY

0.01733

ACCELERATION

0.29637

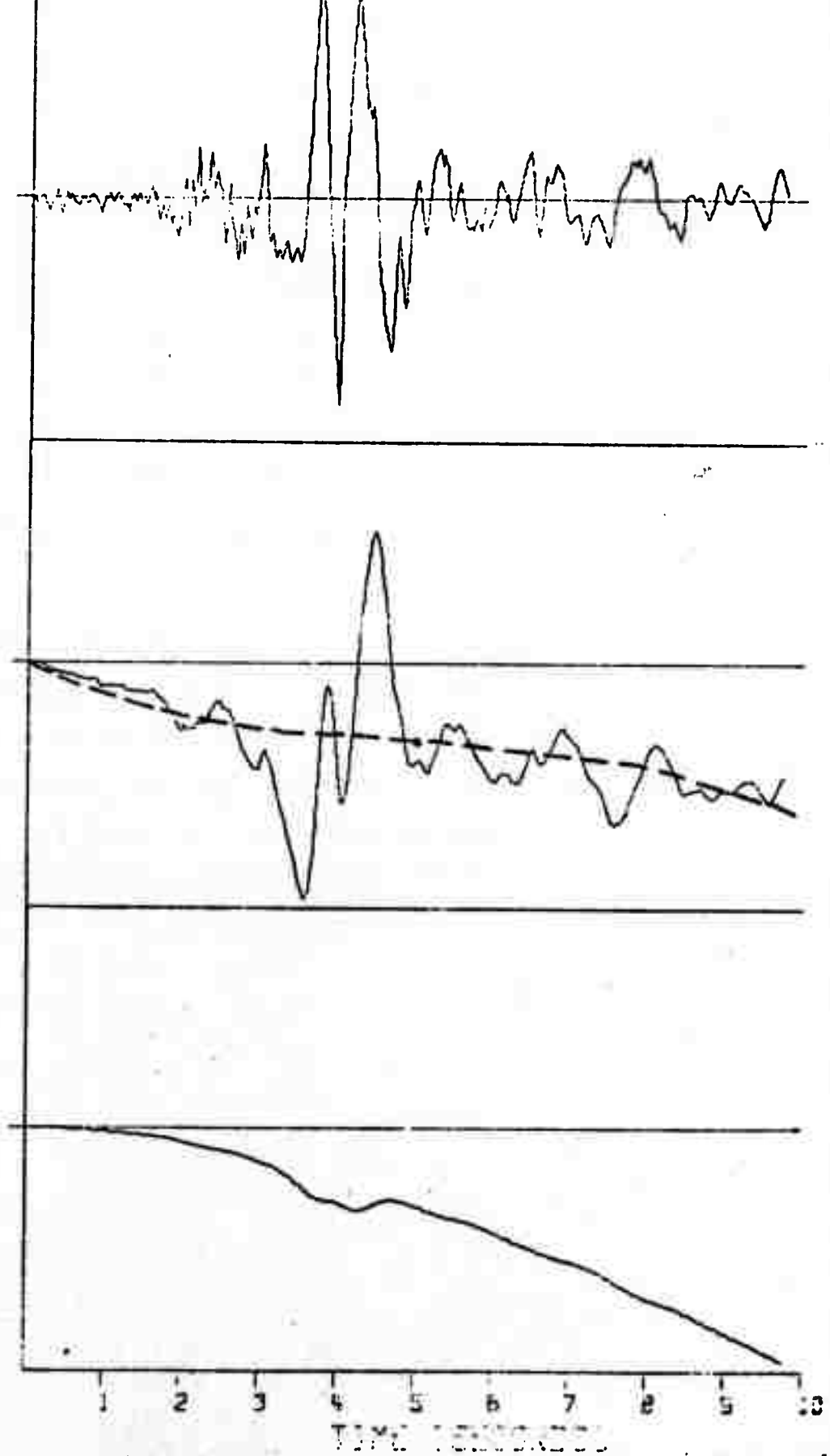


FIGURE III-6

UNCORRECTED VELOCITY TRACE (FITTED CORRECTION CUBIC SHOWN WITH IT) AND RESULTANT DISPLACEMENT TRACE

VEL. COR. DATA STARTS AT 0.0 ENDS AT 9.875
 VELOCITY CORRECTED WITH A CUBIC WITH THE COEFS 0.0 C0 , -1.340F 01 , 2.265E 00 , -1.488E-01 C1 C2 C3
 ROOTS OF THIS CUBIC ARE 0.0 , ***** , ***** RELATIVE TO START OF RECORD (0.0)
 CRITICAL POINTS OF THIS CUBIC LOCAL MAX.= ***** , ***** LOCAL MIN.= ***** , *****
 *****= No Value Entered INFLECTION PT.= 5.673 , -29.130

FIGURE III-8
 FUNCTIONAL CHARACTERISTICS OF THE
 CORRECTION CUBIC

SECTION IV

AN EVALUATION OF VELOCITY AND DISPLACEMENT TRACES IN COMPARISONS BETWEEN ACCELEROGRAM DATA AND THE SOURCE MODEL

The objective of the processing steps in the previous section is to obtain velocity and displacement traces suitable for comparison with waveforms generated by the source model. It became apparent soon after work began on processing accelerograms that the resultant displacement traces are extremely critical to baseline and velocity correction measures. Several velocity correction schemes were considered and tested in an attempt to find one which would improve details in the traces and minimize the sensitivity of the displacement trace to changes in the processing parameters. The correction scheme involving a cubic fit as described in Section III was found to yield displacements which were sensitive to the choice of starting and terminating points of the fit. Nonfitting processes which use correction quadratics and cubics whose coefficients are determined by constraining them to intersect the velocity trace at specified points also produces results that were sensitive to the choice of these points.

To illustrate these findings, consider the processed accelerogram record, for the $N65^{\circ}E$ component, of the Parkfield earthquake, June 28, 1966, Station #2, Cholame, California in Figures III-5 and IV-1. Figure III-5 shows the results of a cubic correction fitted over the interval [0, 10] as explained in Section III. In Figure IV-1 the correction is fitted to the whole record [0, 44]. Contrasts between the displacement traces illustrate its typically sensitive behavior to the choice of parameters for the fit. On the other hand, the velocity traces remain relatively unchanged. Figures IV-2

1833 56.1T, CHOLAME-SHANNON, CAL., NO. 2, JUN 27 66, 2026PST, N65F

ACCELERATION

0.29739

VELOCITY

0.01976

DISPLACEMENT

0.03701

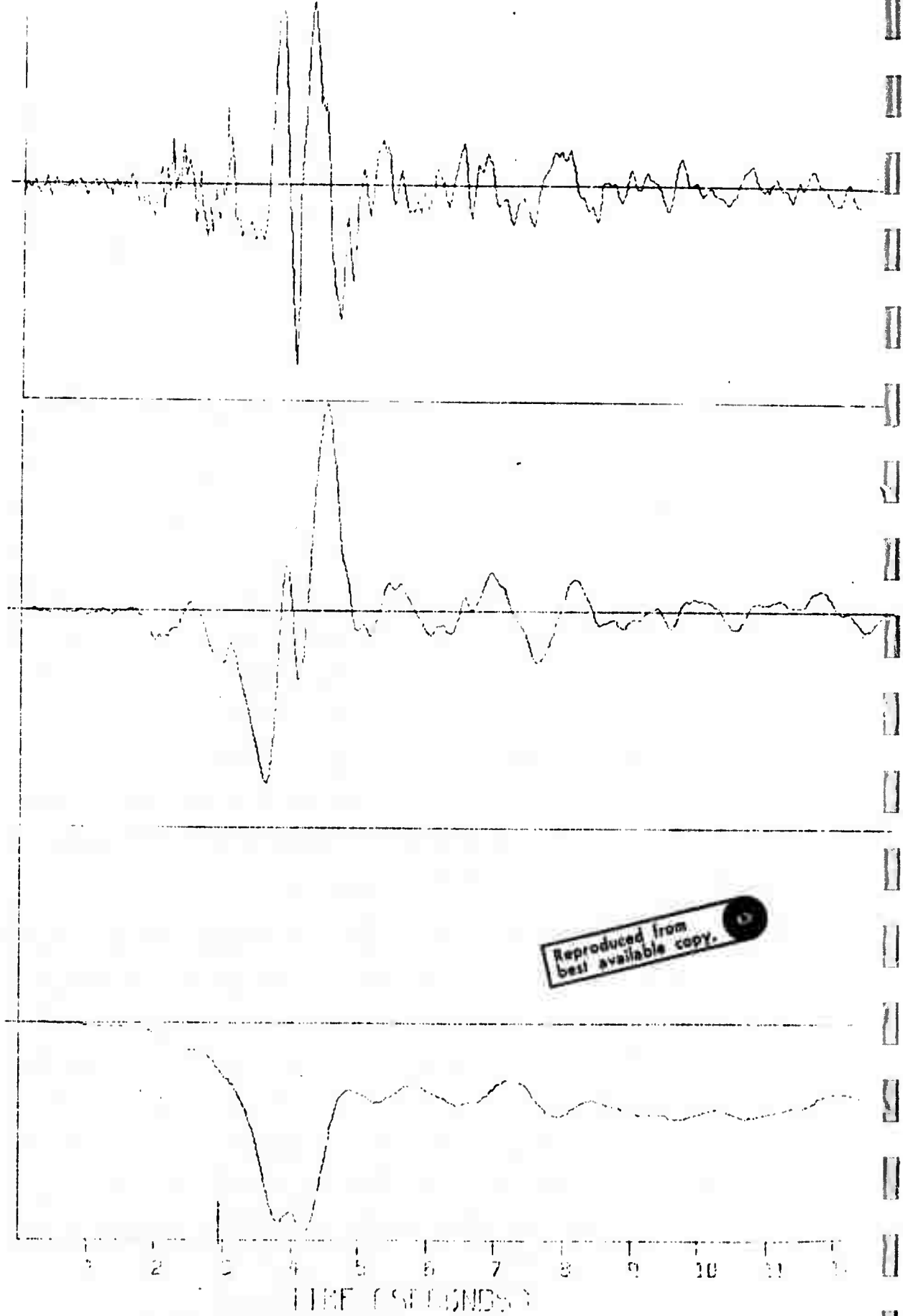


FIGURE IV-1

CORRECTED VELOCITY TRACE (INTERVAL OF FIT [0, 44])
AND RESULTANT DISPLACEMENT TRACE

ACCELERATION

0.11980

VELOCITY

0.02507

DISPLACEMENT

0.03150

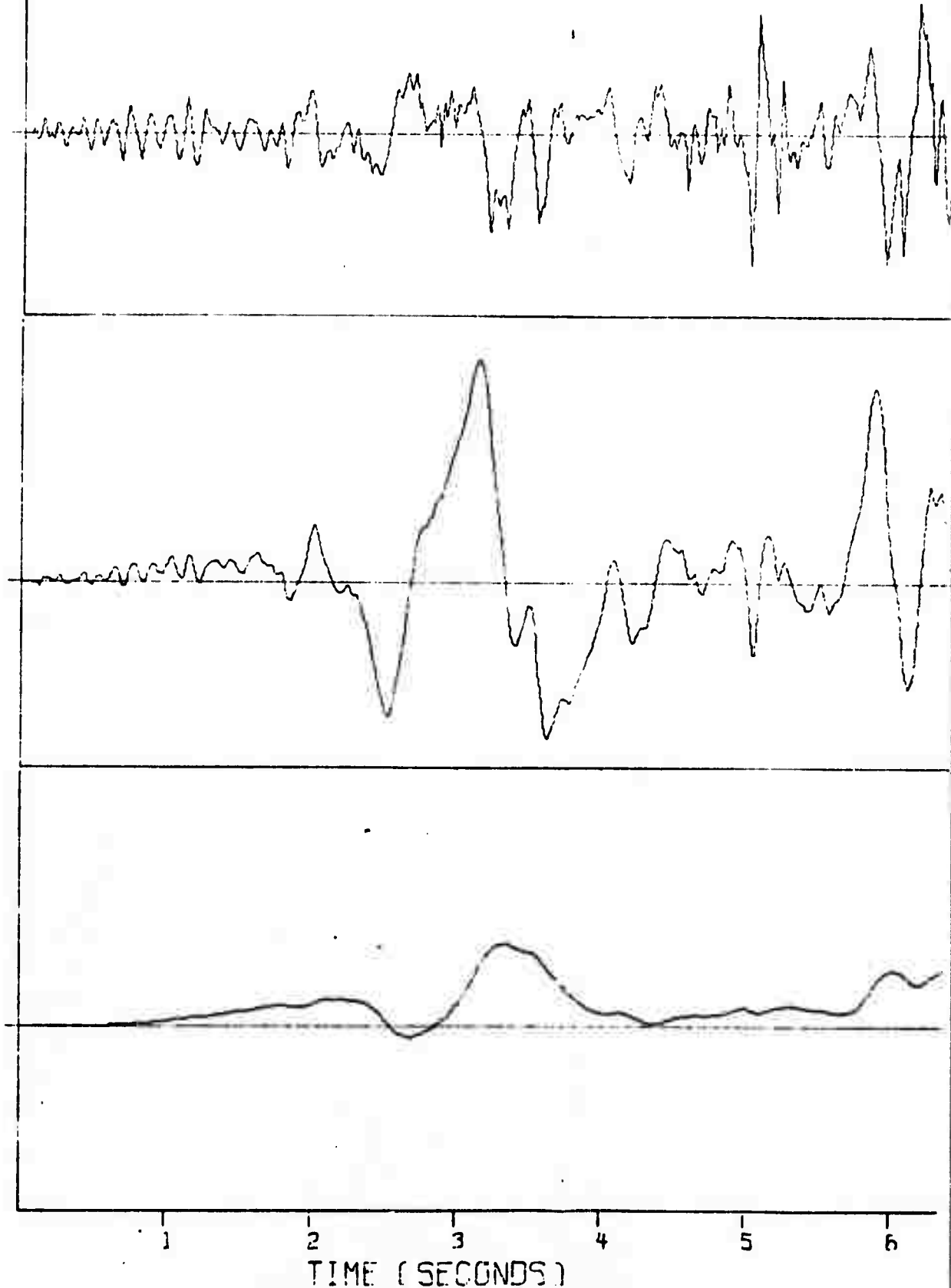


FIGURE IV-2

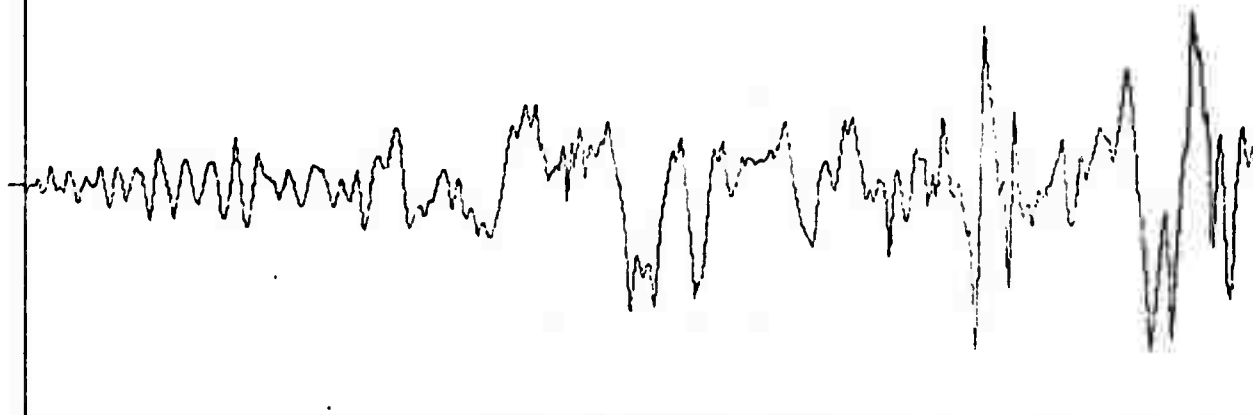
CORRECTED VELOCITY TRACE USING NON-FITTED CUBIC BUT
 CONSTRAINED TO INTERSECT THE UNCORRECTED VELOCITY
 TRACE AT 0, 15, 21, 30 SECONDS AND RESULTANT DIS-
 PLACEMENT TRACE. S74°W ACCELEROGRAM COM-
 PONENT, SAN FERNANDO EARTHQUAKE FEB. 9,
 1971, PACOIMA DAM SITE

and IV-3 are results from a nonfitting process which uses, in this case, a cubic to correct the velocity. The S74^oW accelerogram component recorded at the Pacoima Dam during the San Fernando earthquake, February 9, 1971 is depicted in these figures. The cubic intersected the uncorrected velocity trace at 0, 15, 21 and 30 seconds to yield the results in Figure IV-2 and at 0, 16, 22 and 30 seconds for the results in Figure IV-3. These points were chosen to insure that the corrected velocity trace approached zero late in the record. Again, the resultant displacement traces are quite different, whereas the velocity traces are quite similar.

Thus, it was concluded that, in general, comparisons between velocity traces and theoretical velocity waveforms will be more reliable than comparisons between displacement traces and displacement waveforms.

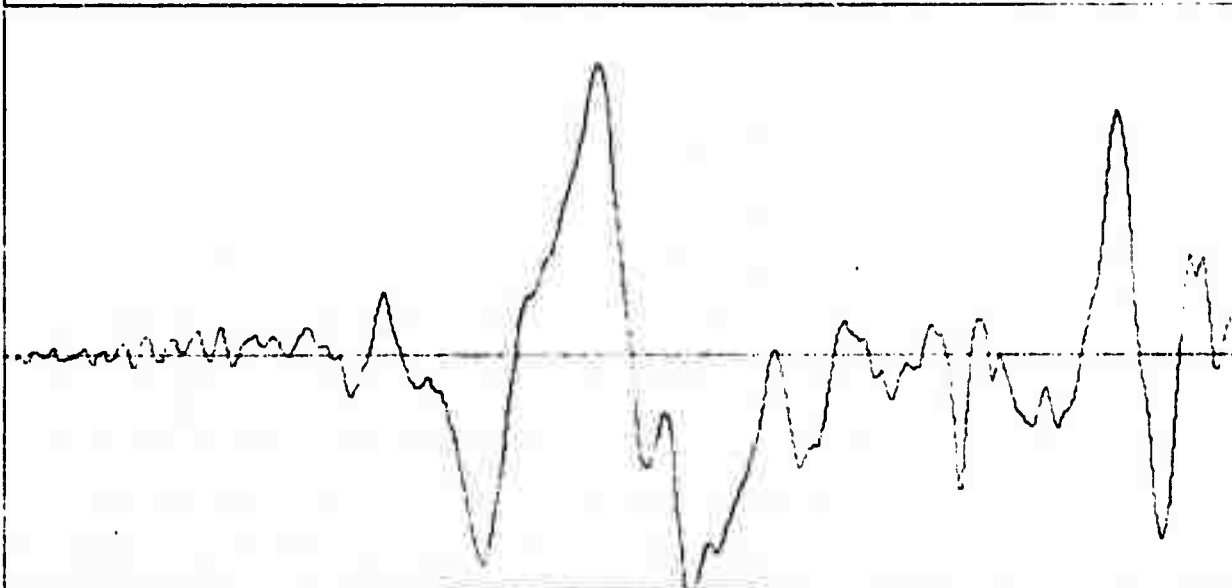
ACCELERATION

0.11980



VELOCITY

0.02728



DISPLACEMENT

0.02593

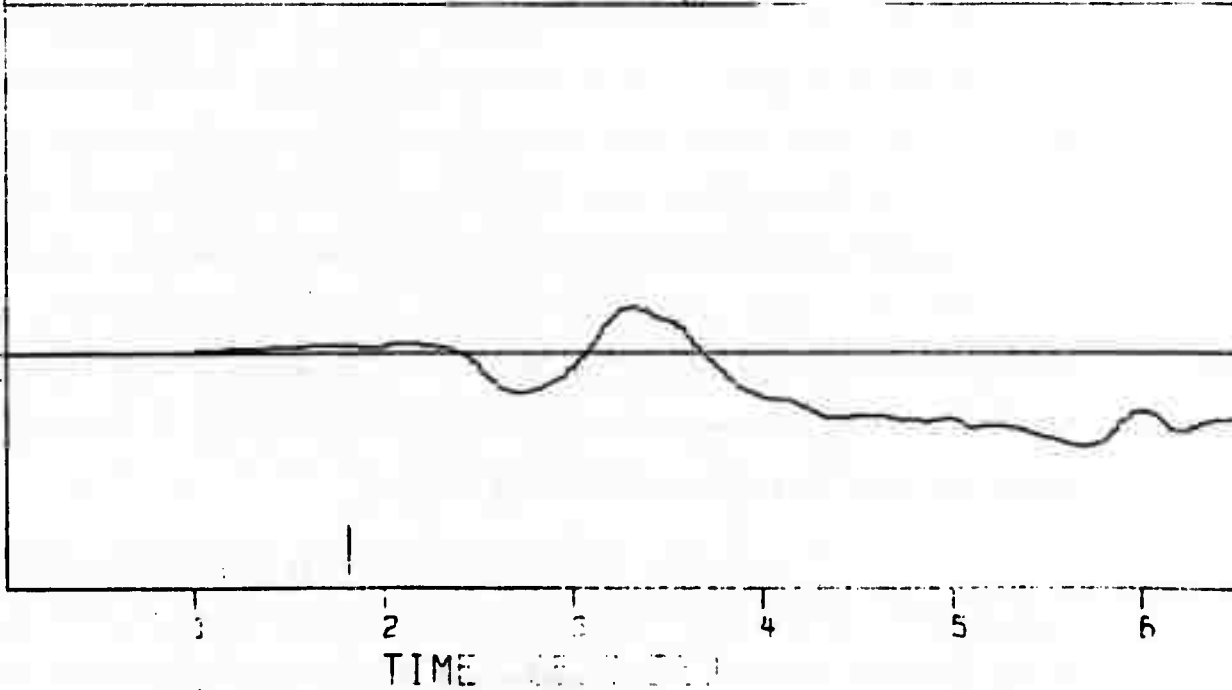


FIGURE IV-3

CORRECTED VELOCITY TRACE USING NON-FITTED CUBIC BUT
CONSTRAINED TO INTERSECT UNCORRECTED VELOCITY
TRACE AT 0, 16, 22, 30 SECONDS AND RESULTANT
DISPLACEMENT TRACE

SECTION V

INTERPRETATION OF THE EARTHQUAKE STRONG-MOTION RECORDS BY A MOVING DISLOCATION MODEL

Application of synthetic displacement waveforms calculated from a moving dislocation model for interpreting the earthquake strong-motion records were first made independently by Aki (1968) and Haskell (1969). Aki takes the Fourier transforms of integrals derived by Maruyama (1963), carries out a numerical integration over the fault plane to obtain the displacement spectrum, and finally returns to the time domain by an inverse Fourier transform. Haskell adopts a somewhat different approach in that he takes the Green's function integrals and evaluates them numerically over the fault plane. For our present purpose Haskell's method is used. According to Haskell, explicit expressions for the three Cartesian components of a displacement time function due to a moving longitudinal or transverse shear dislocation in an infinite homogeneous elastic medium are given in integral forms. Figure V-1 shows the coordinate system and the geometry of the fault plane. The dislocation on the rectangular fault plane is such that a fracture front is formed instantaneously at time $t=0$ across the width W and subsequently propagates at a constant velocity V for a length L along the X axis. At any given point on the fault plane the dislocation increases linearly from 0 at time $t = X/V$ to a constant final value of D_0 at $t = X/V + T$ where T is called the rise time of the dislocation motion.

A computer program for obtaining the displacement waveforms by numerical integration of the Green's function integrals derived by Haskell (1969) has been written. The theoretical displacement waveforms can be

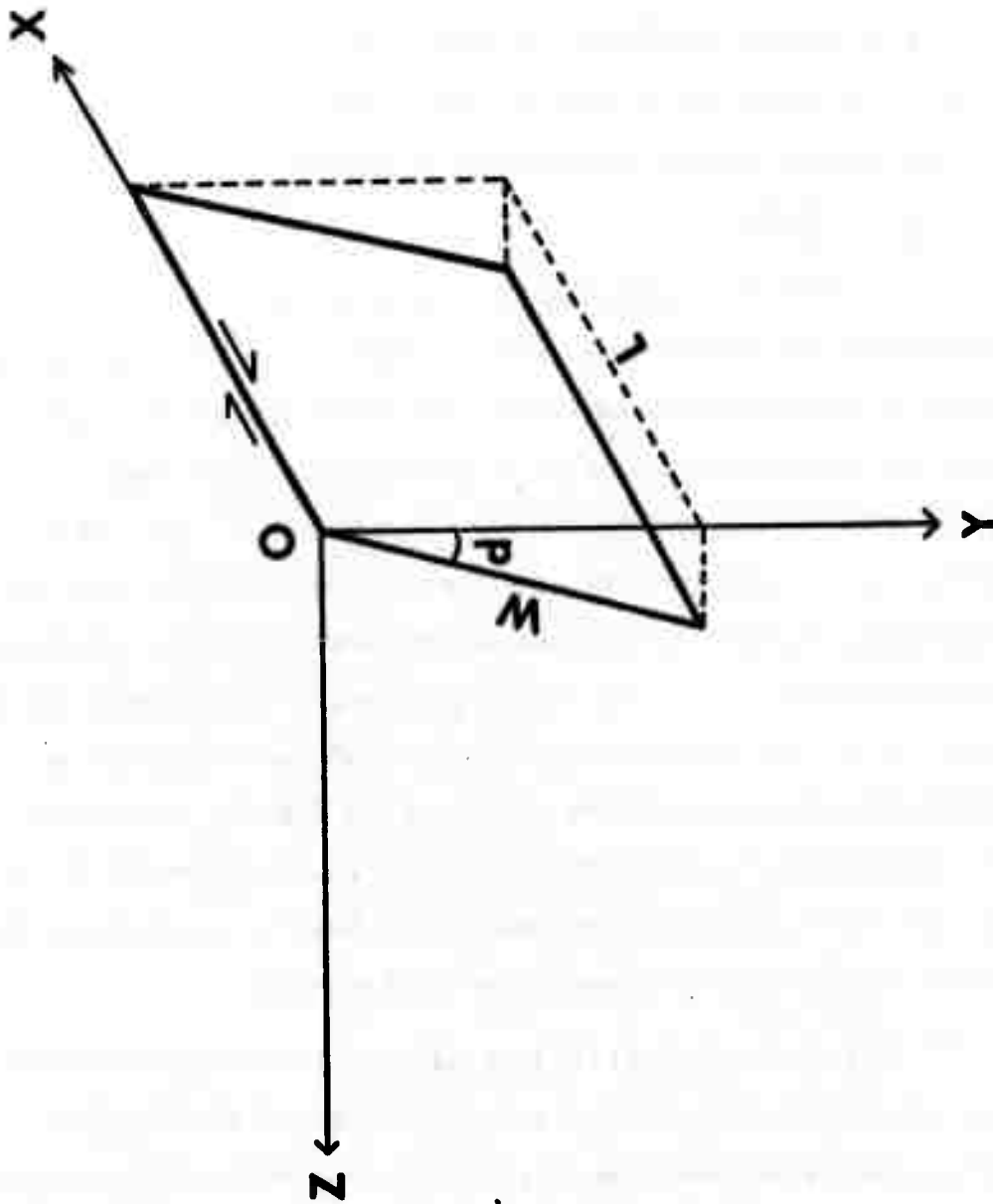


FIGURE V-1
 THE COORDINATE SYSTEM AND THE
 FAULT PLANE GEOMETRY

used for comparison with the experimental displacement waveforms to give an estimate of the dislocation parameters T, V, L, W, and D.

Unfortunately, there exists some serious difficulty arising from the fact that the experimental displacement waveforms have to be derived by integrating the recorded acceleration waveforms twice. As mentioned in a previous section, the resultant experimental displacement waveforms often are highly dependent on the base-line corrections made in the integration process. This results in an unacceptably large uncertainty in the estimates of dislocation parameters.

On the other hand, the experimental velocity waveforms resulting from integrating the recorded acceleration waveforms only once are far less dependent on any particular base-line correction procedure. Thus, more reliable estimates of the dislocation parameters can be obtained by comparing the experimental and theoretical velocity waveforms. The theoretical velocity waveforms to be used for this purpose can be derived from the corresponding theoretical displacement waveforms by numerical differentiation with respect to time. In the process, the earthquake dislocation parameters T, V, L, W, and D are adjusted by trial and error until a reasonable fit of the theoretical to the experimental velocity waveforms is achieved. Sometimes the dimension parameters L (fault length) and W (fault width) are known from other seismological observations such as the ground surface fractures or the distribution of aftershocks.

Remembering that the theoretical velocity waveforms are good only for an infinite homogeneous elastic medium, they will not be strictly comparable to the observed data at the free surface. For the present purpose the effect of free surface will be compensated for by doubling the amplitude of theoretical waveforms computed for the infinite medium.

The accelerograms have been analyzed for two earthquakes in California: the San Fernando earthquake of February 9, 1971 and the Parkfield earthquake of June 28, 1966. The results are described below.

A. THE SAN FERNANDO EARTHQUAKE OF FEBRUARY 9, 1971

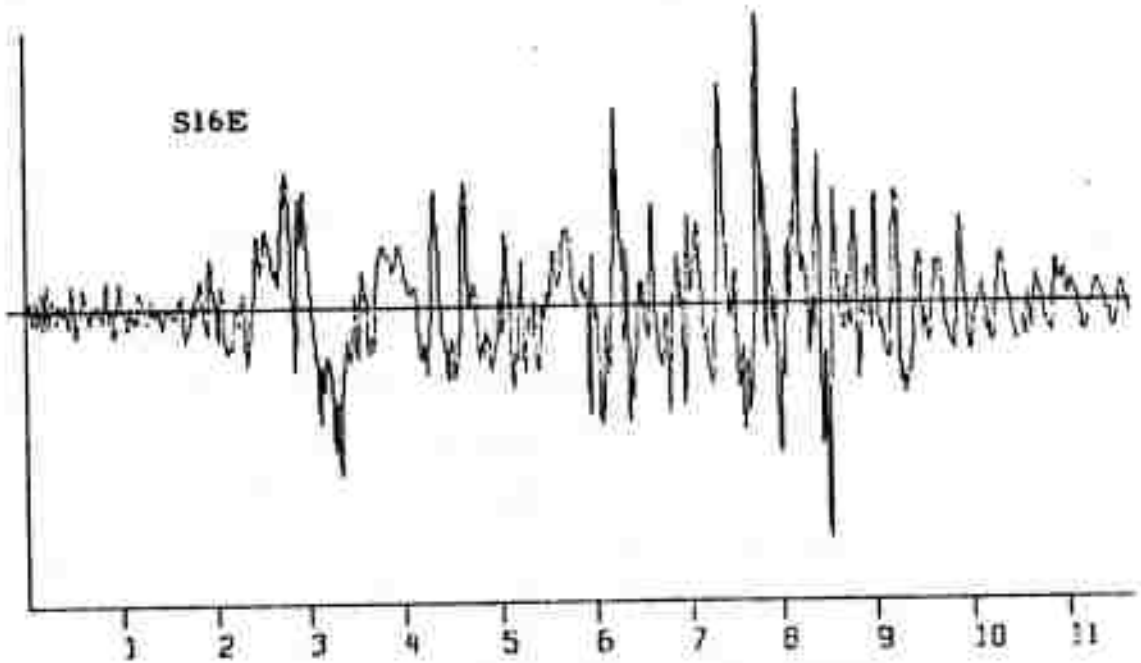
The three-component acceleration traces recorded at the Pacoima Dam accelerograph site during the 6.6 magnitude earthquake are shown in Figure V-2. The waveforms are reproduced from the digitized version of the records provided by the Earthquake Engineering Research Laboratory of the California Institute of Technology. The corresponding velocity waveforms obtained by integration of the acceleration traces are shown by the solid curves in Figure V-3. Unlike the acceleration waveforms which are characterized by the large deflections occurred five seconds or more after the onset of recording, the integrated velocity waveforms have brought out the predominant motion between two and four seconds after the onset of recording. This portion of the velocity waveforms is taken to be directly related to the earthquake dislocation process. This example also clearly suggests that the integrated velocity waveforms are superior to the original acceleration traces as far as interpretation in terms of dislocation is concerned.

The instrumentally-determined focus of the San Fernando earthquake of February 9, 1971 was put at a depth of about 13 km. Surface fracture is centered about 12 km south of the epicenter with an overall trend in $S70^{\circ}E$. Total lateral extent of the surface fracture is about 12 km long. The northern block has been thrust southwestward over southern block. The fault-plane solution gives a well-defined plane striking $N70^{\circ}W$ and dipping 52° in the northeasterly direction (Whitcomb, 1971; Canitez and Toksoz, 1972).

On the basis of this data a dislocation model is constructed as follows: The dislocation surface is taken to have length $L = 16.5$ km, width

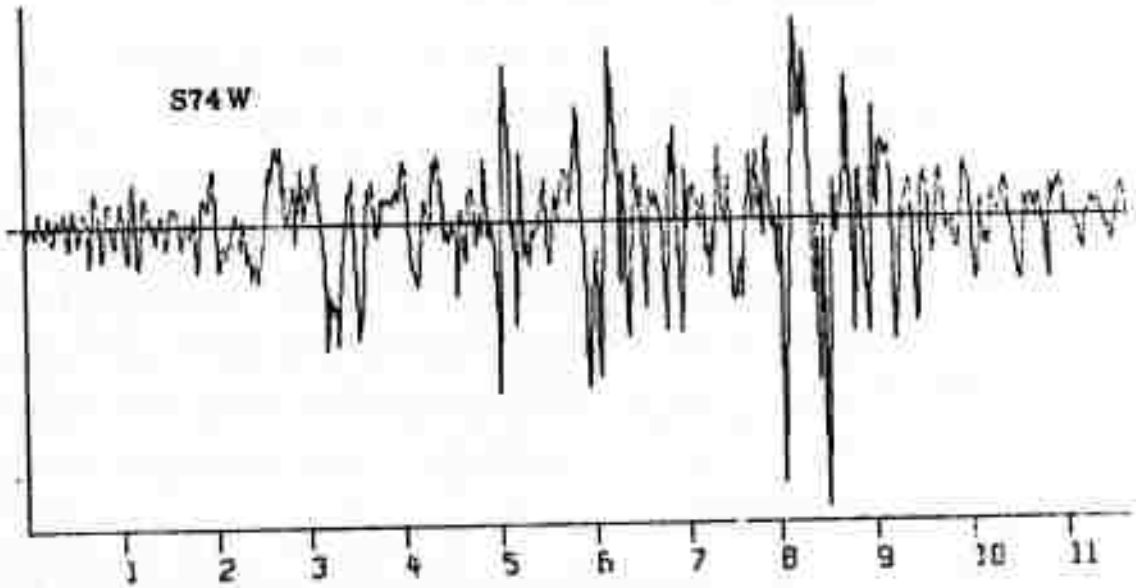
ACCELERATION

0.12000



ACCELERATION

0.12000



ACCELERATION

0.12000

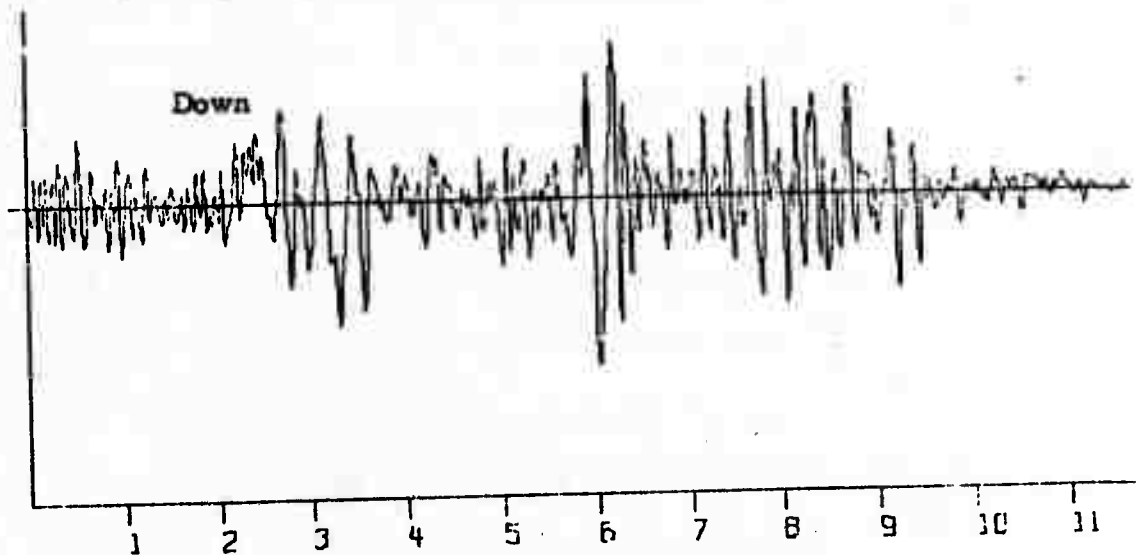


FIGURE V-2
THE ACCELERATION WAVEFORMS DUE TO THE SAN
FERNANDO EARTHQUAKE OF FEBRUARY 9, 1971
RECORDED AT THE PACOIMA DAM

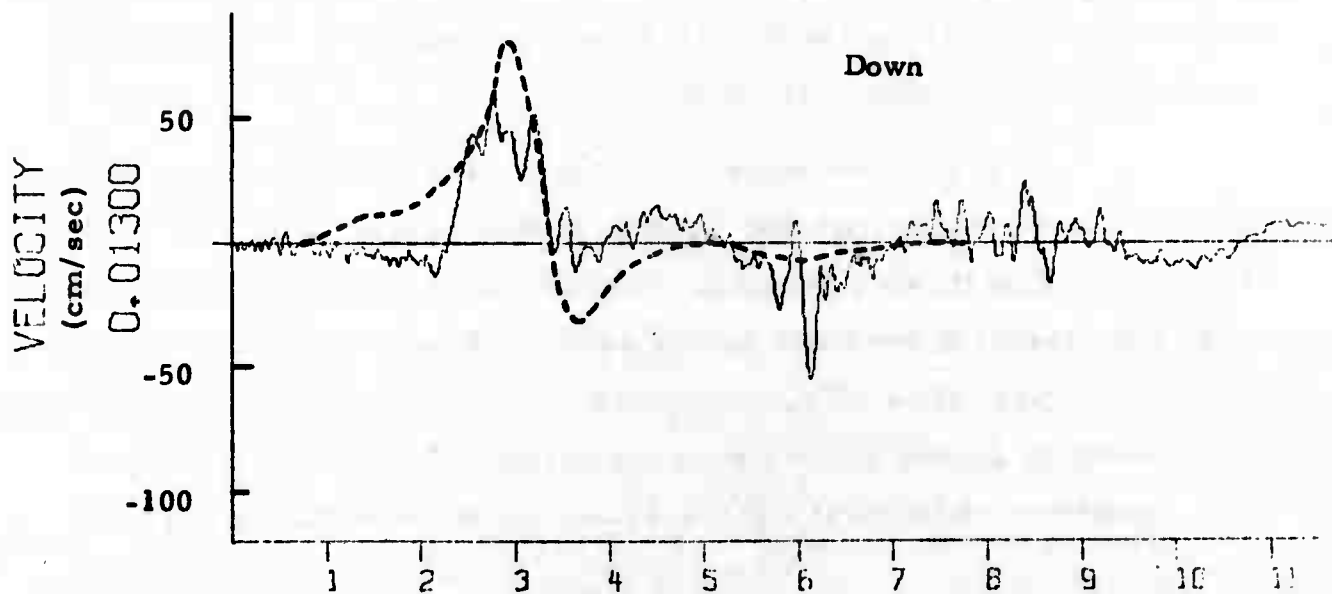
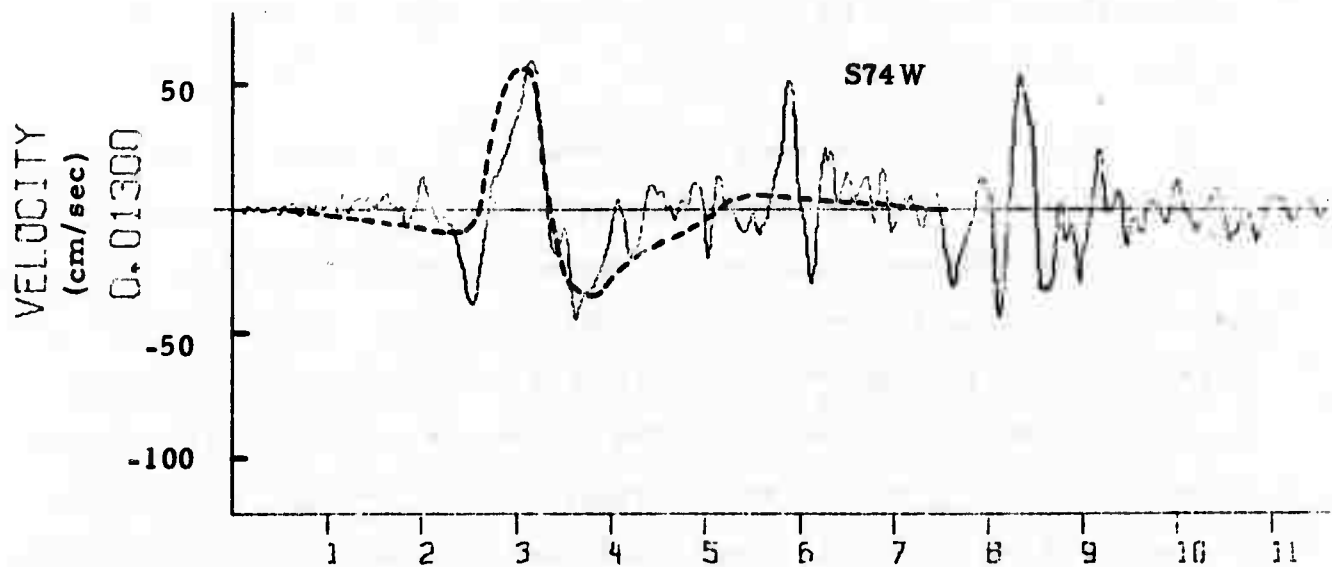
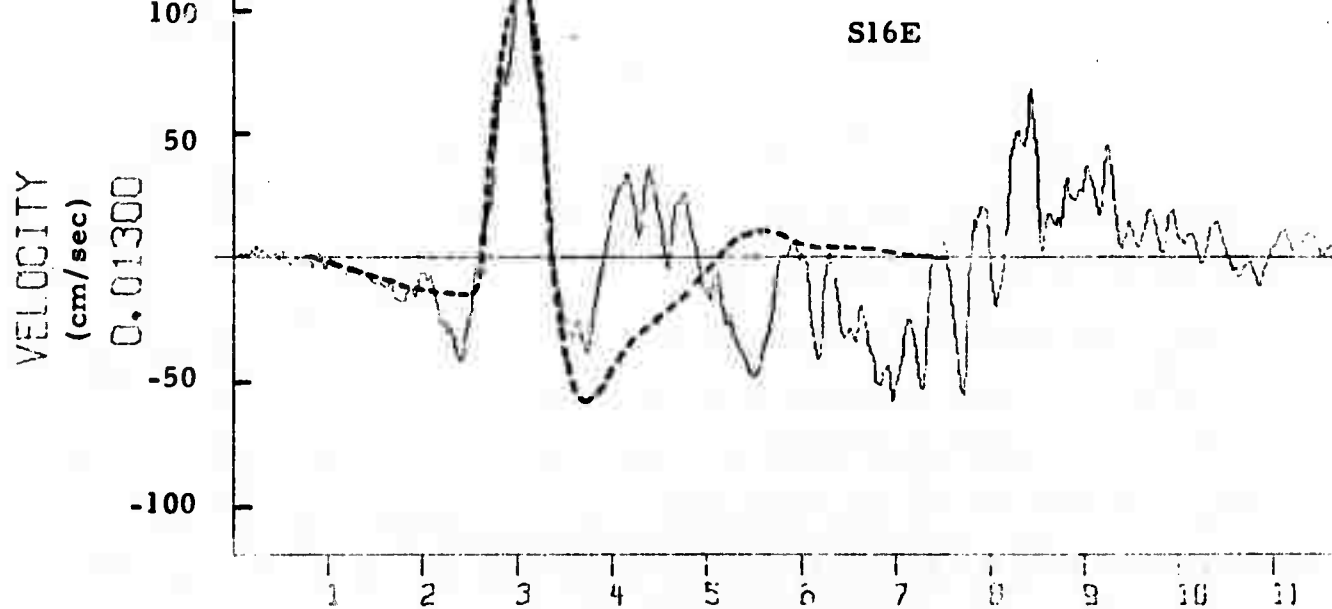


FIGURE V-3
THE OBSERVED (IN SOLID CURVES) AND THE THEORETICAL
(IN DASHED CURVES) VELOCITY WAVEFORMS OF THE
SAN FERNANDO EARTHQUAKE AS SEEN AT THE
PACOIMA DAM V-6

$W = 14$ km and to dip 52° in $N14^{\circ}E$. The upper edge of the dislocation surface is made to coincide with the surface fracture. Then the lower edge would be located at the same depth, i. e., 13 km, as the instrumentally-determined focus. The dislocation is assumed to initiate along the lower edge and propagate up and to the south, past and under the Pacoima Dam accelerograph site, until it intercepts the ground surface in the Sylmar-San Fernando area. Figure V-4 shows the horizontal projection of the modeled dislocation plane as compared to the Pacoima Dam accelerograph site, the epicenters of the main shock and aftershocks, and also the surface fault traces published by Trifunac and Hudson (1971).

Given a constant rupture velocity $V = 3.0$ km/sec, a rise time $T = 0.6$ is found to be appropriate for the earthquake. The resultant theoretical velocity waveforms are the dashed traces in Figure V-3, overlapping the integrated experimental velocity waveforms. The fit between the observed and the theoretical waveforms is remarkably good, especially for the two horizontal components. The final thrust dislocation is estimated to be about 150 cm if the free surface effect is approximated by doubling the amplitudes of the theoretical waveforms computed for an infinite homogeneous medium. A small amount of final strike-slip dislocation, 15 cm is included in obtaining the theoretical waveforms.

It has been suggested on the basis of the fault plane solution and static dislocation model that the final strike-slip dislocation may be as large as the final thrust dislocation. (Canitez and Toksoz, 1971). We have tried this possibility and found that the resultant theoretical velocity waveforms do not have comparable relative amplitudes between the two horizontal components as indicated by the observed velocity waveforms. This is illustrated by the three-component theoretical velocity waveforms shown in Figure V-5. In

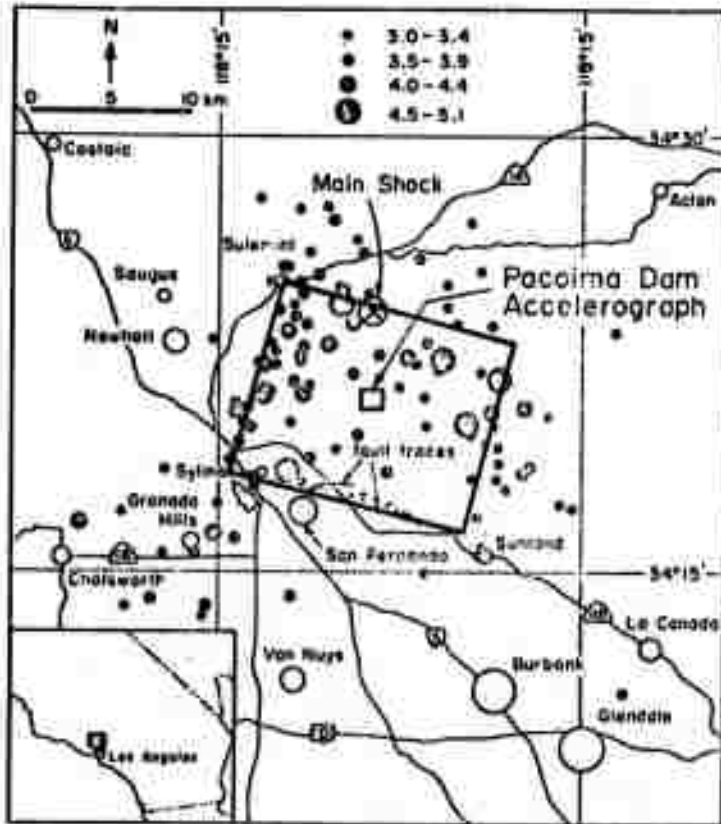


FIGURE V-4
THE HORIZONTAL PROJECTION OF THE ASSUMED FAULT
PLANE AS COMPARED WITH THE LOCATIONS OF THE
PACOIMA DAM ACCELEROGRAPH, THE MAIN SHOCK,
AND THE AFTERSHOCKS

this case, the strike-slip dislocation component is set to be half as large as the thrust dislocation component. The theoretical amplitude ratio of the $S74^{\circ}W$ component versus the $S16^{\circ}E$ component amounts to only 1:4 in the present case. This falls far below the actual ratio of about 1:2 as revealed by the upper two traces in Figure V-3. Thus, on the basis of the preceding evidence we concluded that the dynamic dislocation process associated with the San Fernando earthquake is predominated by thrust motion.

The dislocation parameters determined above can be combined to give an estimate of the seismic moment by:

$$M_0 = \mu DWL \quad (V - 1)$$

where μ is the modulus of rigidity, D is the average dislocation across the fault surface which has a width of W and length L . Taking the values mentioned above, namely, $D = 150$ cm, $W = 14$ km, $L = 16.5$ km and setting $\mu = 3 \times 10^{11}$ dyne cm^{-2} , we find $M_0 = 10.4 \times 10^{25}$ dyne cm. This last value is smaller than the one estimated from static displacement data 16.4×10^{25} dyne cm, but is larger than the one determined from surface-wave data, 7.5×10^{25} dyne cm, as reported by Canitez and Toksoz (1971).

In view of the highly simplified model of the actual dislocation process, the overall results are indeed very encouraging. However, we also hasten to point out that only a relatively small portion in the beginning of the records has been explained. There still exists a large later portion during which the maximum acceleration occurs which is left completely unexplained. Inclusion of a free surface and layering of the medium in the model may help explain the latter portion of the record.

B. THE PARKFIELD EARTHQUAKE OF JUNE 28, 1966

We have also applied the moving dislocation model to interpret the Parkfield Station 2 record. Figure V-6 shows the location of Station 2

the Parkfield Station 2 record. Figure V-6 shows the location of Station 2 with respect to the San Andreas Fault and the surface cracks associated with the earthquake. The instruments of Station 2 were situated only about 80 meters from the fault trace. Only the vertical and one horizontal component available is reproduced in the upper part of Figure V-7 from the digitized version of the original waveform. The integrated velocity waveform is shown by the solid trace in the lower part of Figure V-7. The dashed trace is the theoretical velocity waveform corresponding to a right-lateral strike-slip dislocation propagating southeastward starting from a point about 8 km to the northwest of Station 2 and ending at a point 2 km to the southeast of Station 2. The width of the dislocation surface W is set to equal 6 km. To the extent that the free surface boundary conditions are approximately satisfied by adding an image source, we may regard the plane bisecting the fault width as representing the free surface and the half of the dislocation surface lying about this level as representing the image of a fault whose real dimensions are 10 km by 3 km. Because of the closeness of the observation point to the fault plane, i. e., 0.08 km, we use Simpson's method of numerical integration over a grid of 100 x 60 points covering the dislocation surface for numerical integration. With a given rupture velocity of 2.2 km/sec the rise time is found to be about 0.9 sec. The resultant theoretical velocity waveform, as shown by the dashed trace, fits very well with the integrated waveform, as shown by the solid trace in the lower part of Figure V-7. The final right-lateral strike-slip dislocation is determined to be about 200 cm.

Haskell (1969) has proposed a source time function consisting of two discrete ramp steps for this earthquake. The time duration for the dislocation to reach its final value was determined as 0.84 sec in this case. Thus, our value of 0.9 sec for the rise time is in good agreement with Haskell's result. As mentioned earlier, Aki (1968) also has interpreted the

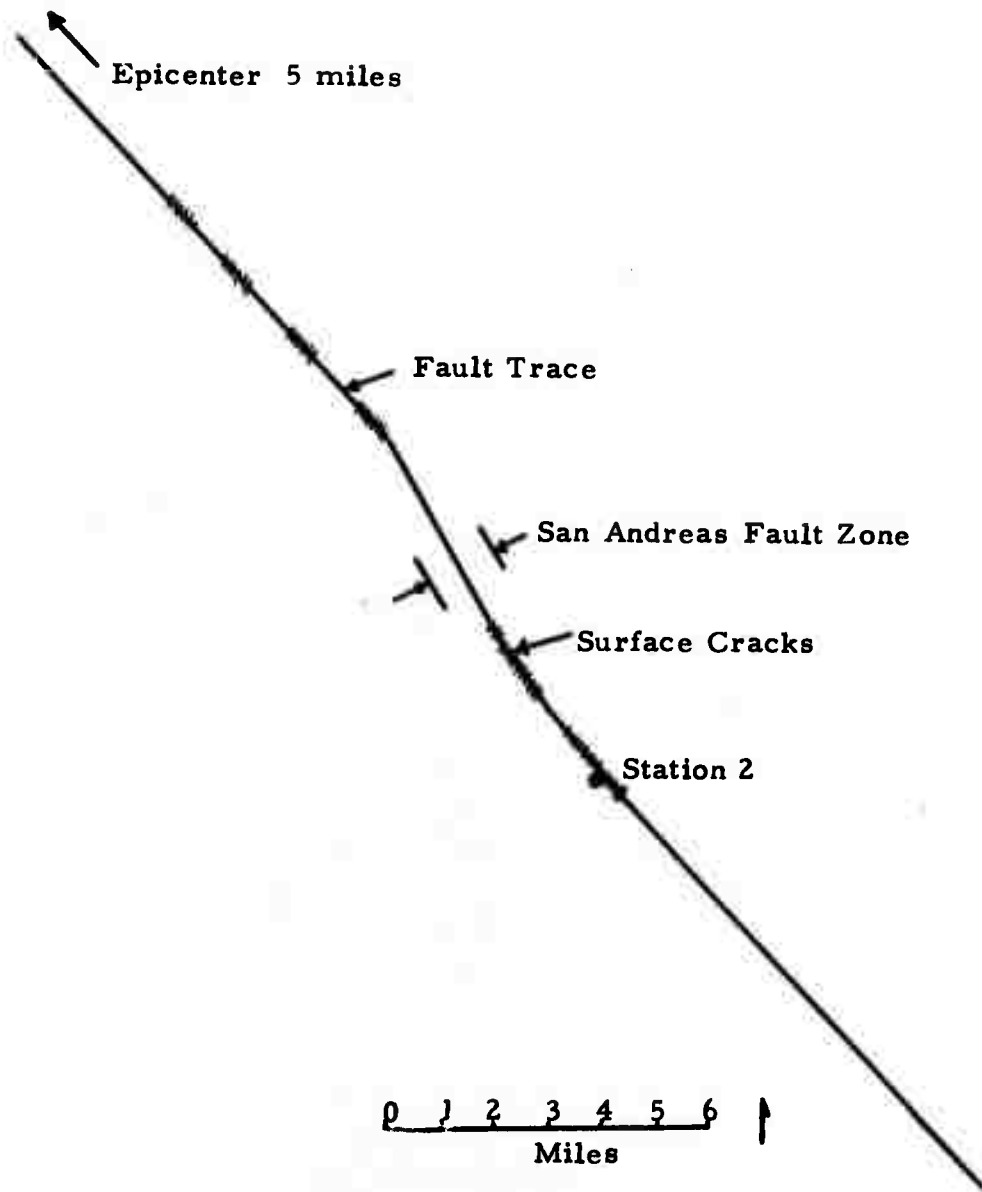


FIGURE V-6

**THE LOCATION OF STATION 2 ACCELEROGRAPH WITH RESPECT
TO THE SAN ANDREAS FAULT TRACE AND THE SURFACE
CRACKS DUE TO THE PARKFIELD EARTHQUAKE OF
JUNE 28, 1966**

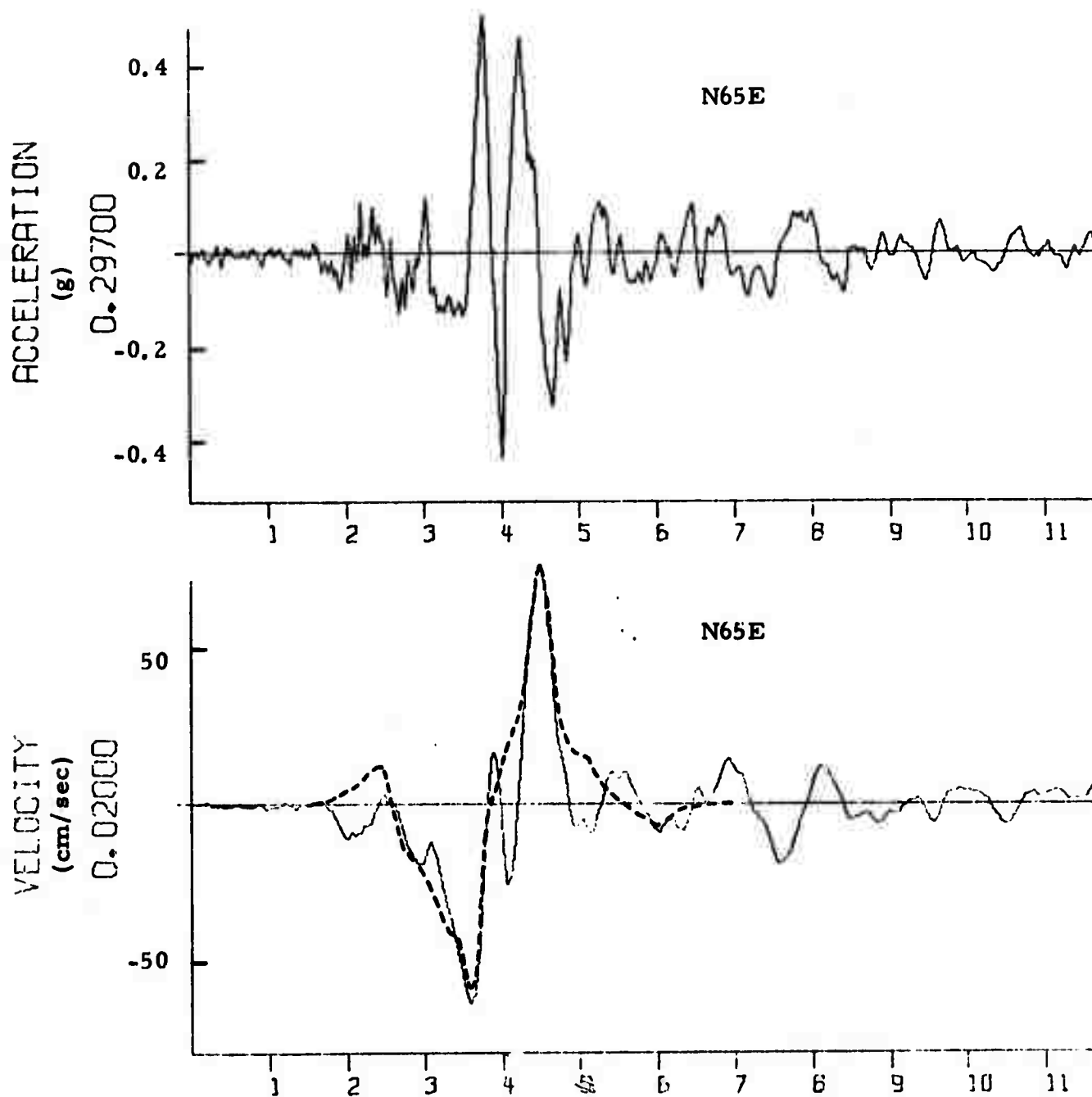


FIGURE V-7

A. THE OBSERVED HORIZONTAL ACCELEROGRAM (N65°E)
 AT STATION 2 DURING THE PARKFIELD EARTHQUAKE
 OF JUNE 28, 1966; B. THE CORRESPONDING
 OBSERVED AND THEORETICAL VELOCITY
 WAVEFORMS

same record using a Fourier synthetic technique. He has estimated the final dislocation to be about 60 cm. Thus, our value of 200 cm is more than three times larger than Aki's estimate. This discrepancy results largely from the fact that Aki uses a step source time function whereas we use a ramp function. To illustrate this point, we have computed the theoretical velocity waveforms for two different values of rise time. Figure V-8 shows the three-component velocity waveforms calculated by using the following dislocation parameters: $L = 6.4$ km, $W = 3.0$ km, $V = 2.2$ km/sec, $D = 200$ cm, $T = 0.8$ sec. These waveforms are to be compared with the corresponding ones shown in Figure V-9 which are computed with all parameters unchanged except the rise time has been reduced from 0.8 sec to 0.4 sec. It is apparent that a reduction of rise time by half has caused the theoretical waveforms in both horizontal components to substantially shorten the pulse durations on one hand and to nearly double the pulse amplitudes on the other. With a very small rise time approaching a step function the increase of theoretical velocity amplitudes would be even greater. Thus, given the observed waveforms, the inferred final dislocation will decrease with decreasing rise time.

Because there are so many parameters involved in this type of analysis the outcome is necessarily non-unique. However, if the integrated velocity waveforms are of sufficiently good quality, some proper limits for the parameters can be established. For instance, if the theoretical waveform of the $N65^{\circ}E$ component shown in Figure V-9 is compared with the observed waveform shown previously in the lower part of Figure V-7 it immediately becomes clear that a rise time of 0.4 sec is too small to account for the observed pulse duration.

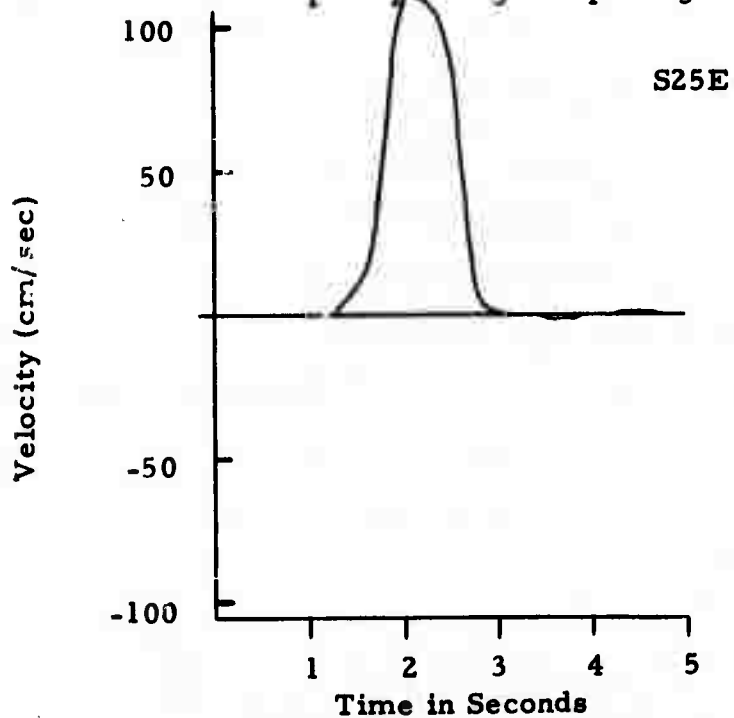
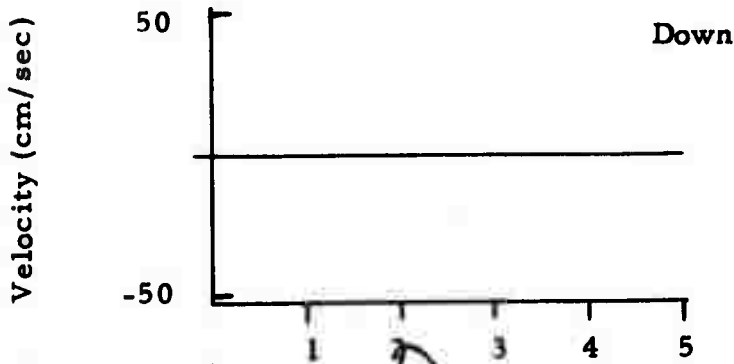
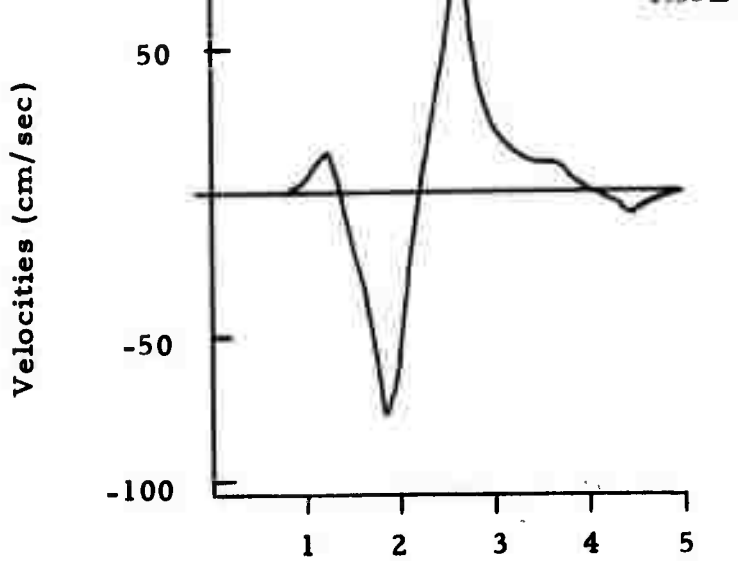


FIGURE V-8

THE THEORETICAL VELOCITY WAVEFORM FOR A MOVING STRIKE-SLIP DISLOCATION WITH $W = 3.0$ km, $L = 6.4$ km, $V = 2.2$ km/sec, $T = 0.8$ sec, $D_0 = 200$ cm

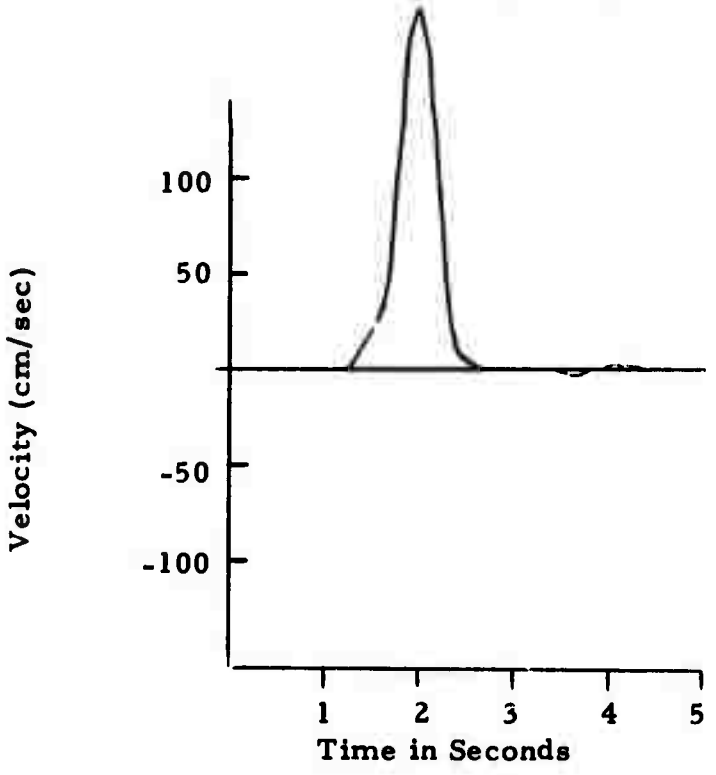
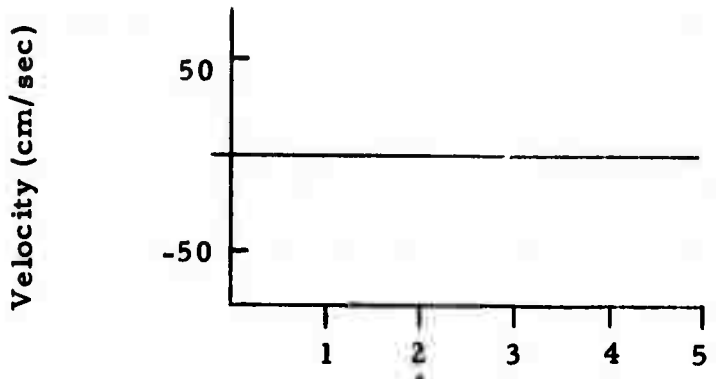
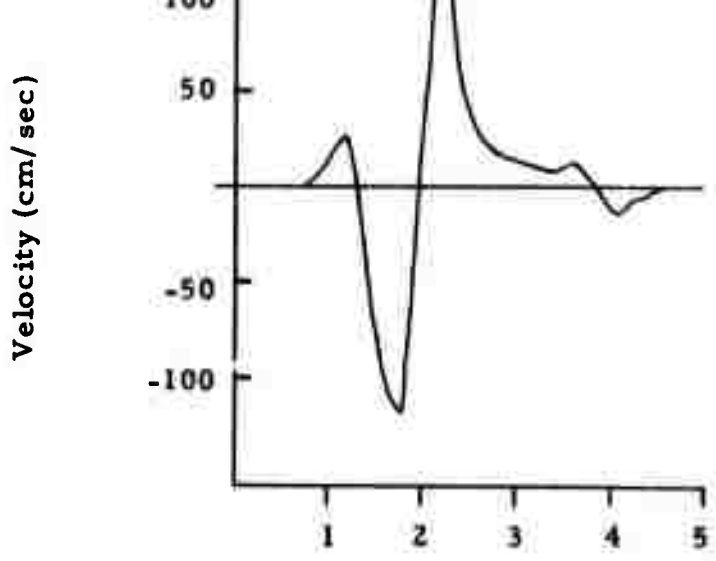


FIGURE V-9

THE THEORETICAL VELOCITY WAVEFORM FOR A MOVING STRIKE-SLIP DISLOCATION WITH $W = 3.0$ km, $L = 6.4$ km, $V = 2.2$ km/sec, $T = 0.4$ sec, $D_o = 200$ cm

The seismic moment of the Parkfield earthquake has been determined as 1.4×10^{25} dyne cm from surface-wave data by Tsai and Aki (1969). By setting $\mu = 3 \times 10^{11}$ dyne cm^{-2} and using the parameters estimated above, namely, $L = 10$ km, $W = 3$ km, $D = 200$ cm, we obtain a seismic moment $M_0 = 1.8 \times 10^{25}$ dyne cm. The agreement of the two values is excellent. The fault length L of the earthquake has been determined as 30 to 37 km from various sources of information [Brown and Vedder, 1967; Filson and McEvelley, 1967; Tsai and Aki, 1969]. This is more than three times larger than the 10 km inferred from the strong-motion record at Station 2. If we use this fault length and the seismic moment mentioned above then the average final dislocation over the whole length will amount to only one third of the 200 cm estimated in the present study. This strongly suggests that the dislocation along the fault associated with the Parkfield earthquake is not uniform but concentrated in the 10 km portion near the southeastern tip of the fault.

SECTION VI

EVALUATION OF TWO DISLOCATION TIME FACTORS

In this section two time functions, a linear ramp function and an exponential ramp function, for dislocation are evaluated. These two dislocation time functions are plotted in Figure VI-1. The linear ramp function has been investigated by Haskell (1969) with some success. The exponential ramp function was proposed by some investigators as an alternative to the linear ramp since this function has similar characteristics and is continuous for all time greater than zero. Contrasts between the velocity functions associated with these mechanisms raised doubts, however, concerning the quality of resultant waveforms, especially at relatively distant observation points.

The evaluation was based on the comparison between theoretical waveforms and first motion pulses in velocity traces obtained from accelerograms recorded at the Pacoima Dam site during the San Fernando earthquake of February 9, 1971. The velocity traces are shown in Figure V-3. Although some of the model parameters were determined from field observations for this earthquake, the remaining parameters were adjusted by trial and error. Particular attention was given to the effect of different rise times on the theoretical waveforms. As described in Section V, satisfactory agreement between the linear ramp results in Figure VI-2 and first motion pulses was obtained for 0.6 second rise time.

Figures VI-3 and VI-4 depict velocity waveforms for the exponential ramp at 0.3 second and 0.6 second rise time, respectively. The observations from these two cases and from other cases for the exponential

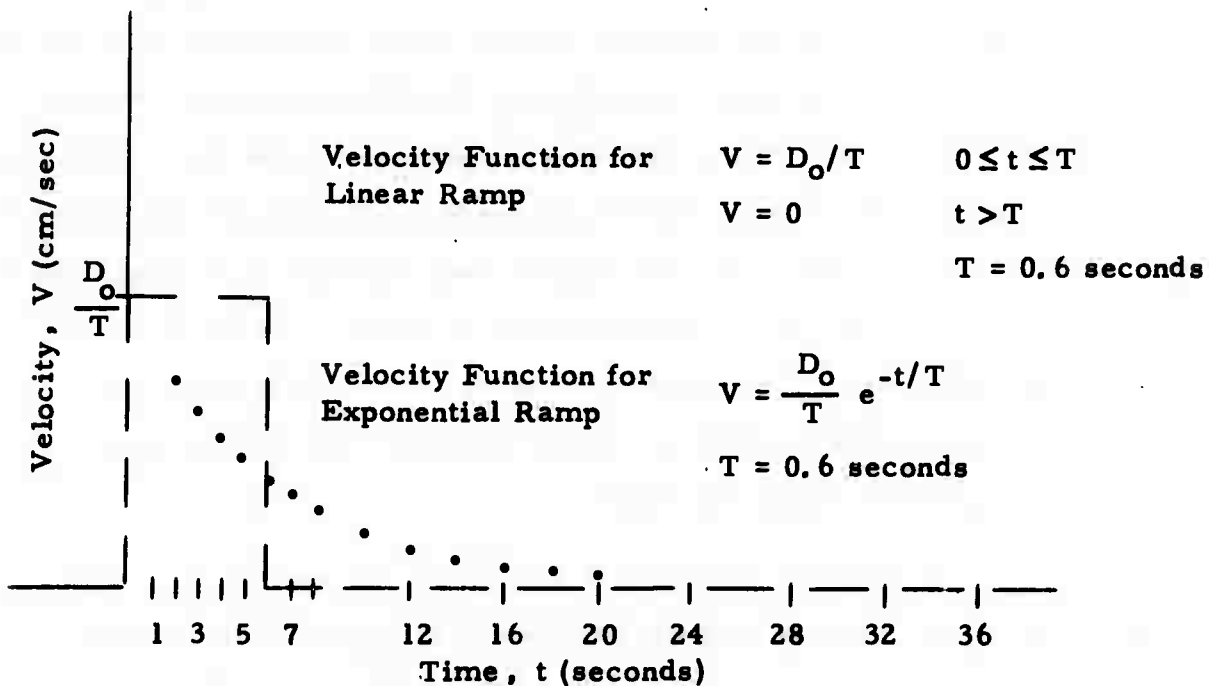
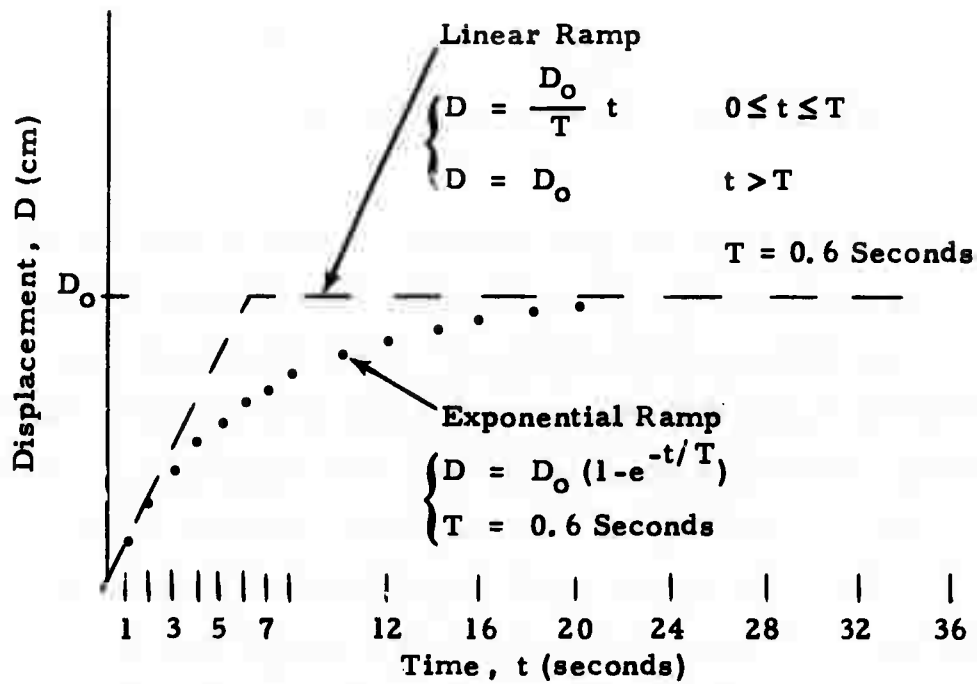


FIGURE VI-1

LINEAR AND EXPONENTIAL RAM DISLOCATION TIME
FUNCTIONS AND THEIR ASSOCIATED VELOCITY FUNCTIONS

PACOIMA DAM SITE: SAN FERNANDO EARTHQUAKE

S16E

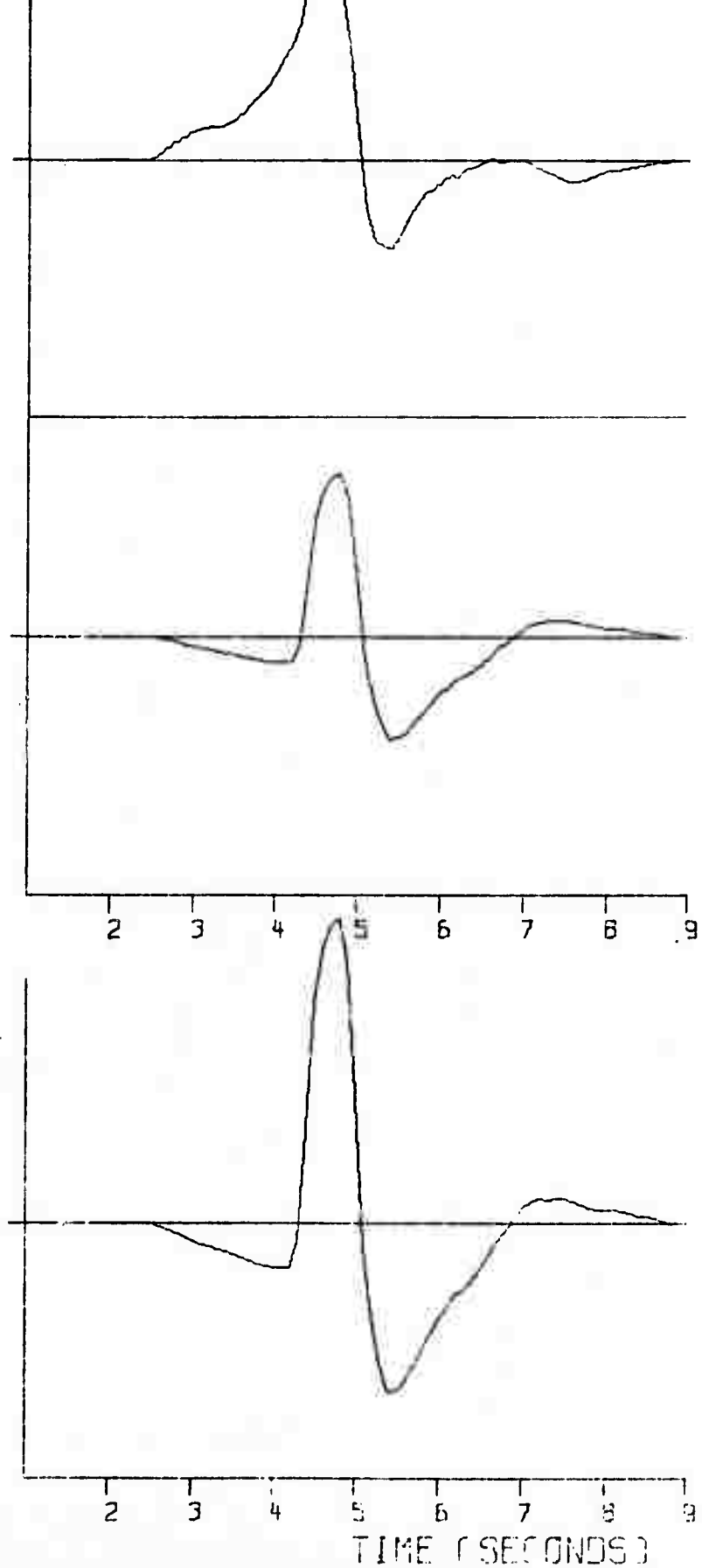
-0.02000

S74W

-0.02000

DOWN

-0.02000



Reproduced from
best available copy.

FIGURE VI-2

THEORETICAL VELOCITY WAVEFORMS, LINEAR RAMP
FUNCTION WITH RISE TIME = 0.6 SECONDS

VI-3

VELOCITY WAVEFORMS FOR THE EXPONENTIAL RAMP FUNCTION, RISE TIME = 0.3 SECS

VERT

0.02000

S74W

0.02000

S16E

0.02000

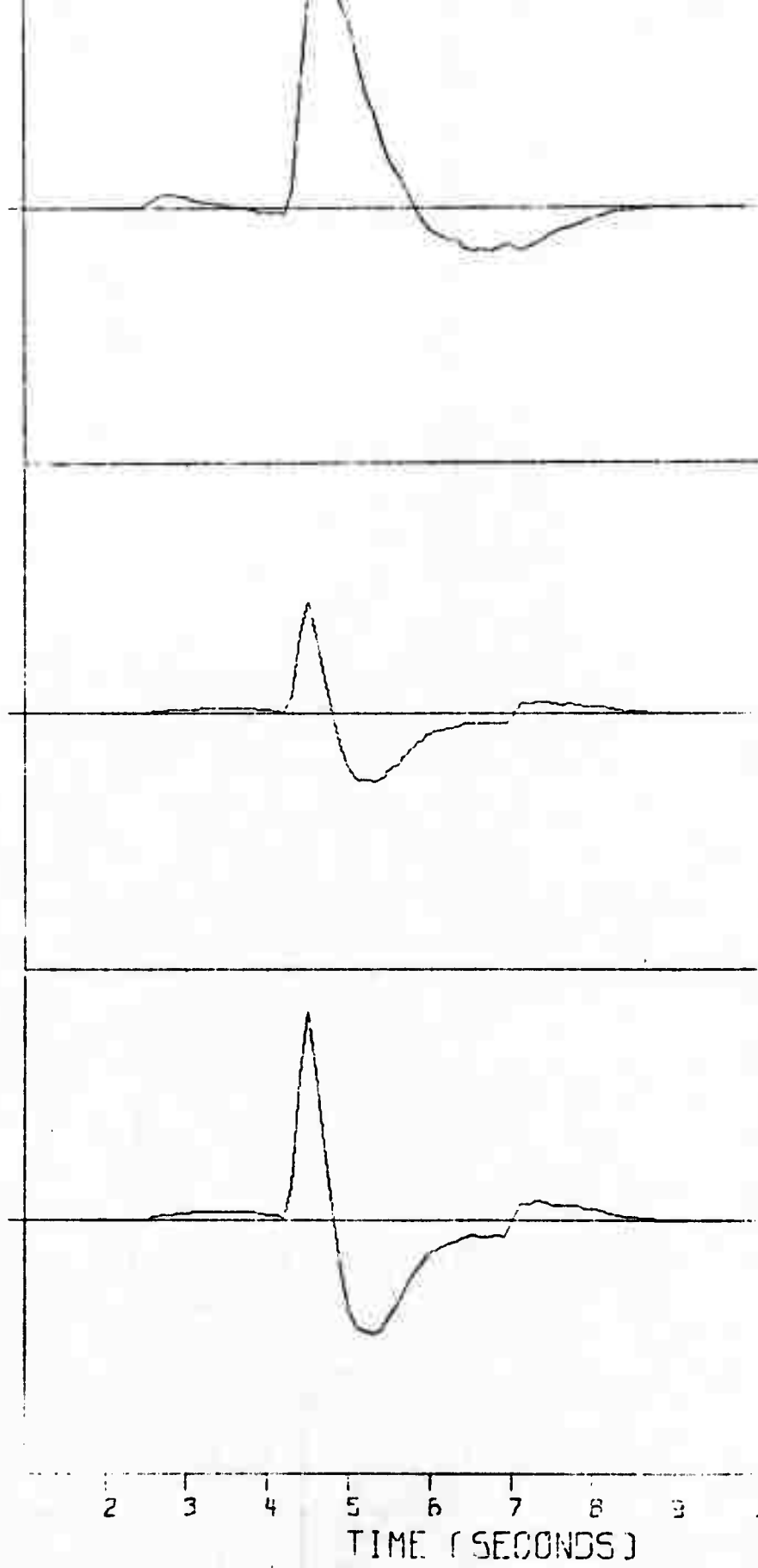


FIGURE VI-3

THEORETICAL VELOCITY WAVEFORMS, EXPONENTIAL RAMP FUNCTION WITH RISE TIME = 0.3 SECONDS

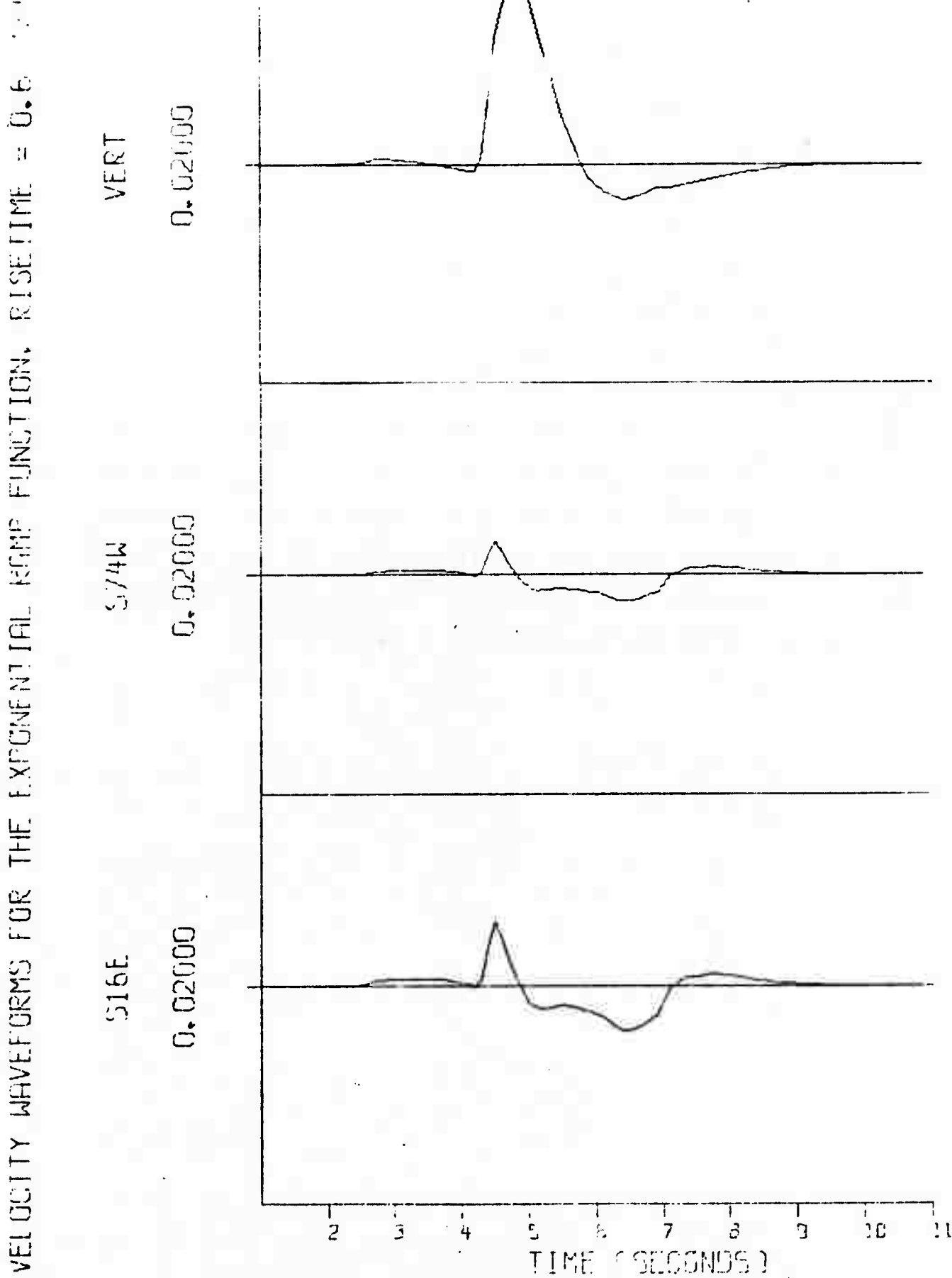


FIGURE VI-4

THEORETICAL VELOCITY WAVEFORMS, EXPONENTIAL
RAMP FUNCTION WITH RISE TIME = 0.6 SECONDS

VI-5

ramp are fourfold: 1) Amplitudes of first motion pulses are generally smaller than those for the linear ramp. Since the relationship between amplitude and final displacement, D_0 , is linear, the results in Figure VI-4, for example, would require fault dislocations of six meters, approximately four times the accepted value. 2) First motion pulses are followed by downward swings whose durations become larger and tend to dominate the waveform as the rise time is increased. 3) Changes in the rise time do not affect that upswing pulse widths which for these cases are too short to fit the observation. 4) While the arrivals of pulses for the $S16^{\circ}E$ and $S74^{\circ}W$ components can be made to coincide with those observed in Figure V-3, the vertical pulse consistently lags behind its observed counterpart. Apparently, the gradual decay of the exponential velocity function is the cause of these ill effects in the resultant velocity waveforms. Thus, based on these observations, the exponential ramp is regarded as inferior to the linear ramp.

SECTION VII

SUMMARY

In summing up our accomplishments to date concerning the analysis of near-field earthquake strong-motion records, the following remarks are appropriate:

- Major programs performing the calculations of theoretical waveforms, the processings of digitized strong-motion records have been written, checked, and are operational. All the computer programs related to this project have the capability to make Calcomp plots as well as printer plots for visual inspection.
- A file of fifty-one three component digitized strong-motion records has been set up in a unified format and stored on a nine-track magnetic tape. This has greatly reduced the time and labor required in data handling, thus providing excellent conditions for more rapid data processing in the future.
- It was found that a linear and a cubic least squares corrections of the acceleration and the integrated velocity waveforms, respectively, can result in reasonably reliable experimental velocity waveforms for interpretation using a moving dislocation model.

- The one-time integrated velocity waveforms are far less sensitive to various schemes of numerical integration and baseline corrections than the corresponding twice integrated displacement waveforms. Thus, it is suggested that comparison of the experimental and the theoretical waveforms can be more reliably carried out at the velocity level.
- Interpretation of the accelerograms at the Pacoima Dam site recorded during the San Fernando earthquake of February 9, 1971 using the moving dislocation model yields the following picture of the dislocation process associated with the earthquake: The rupture was initiated at the depth level of the instrumentally-determined focus and then propagated up and to the south, past and under the Pacoima Dam accelerograph site along a fault surface dipping at 52° . The final dislocation and the time to reach it are estimated as 150 cm and 0.6 sec, respectively. The seismic moment estimated using the determined dislocation parameters is 10.4×10^{25} dyne cm.
- The dislocation process associated with the Parkfield earthquake of June 28, 1966 as inferred from analysis of the Station 2 accelerograms using the moving dislocation model is as follows: The right-lateral strike-slip dislocation amounted to about 200 cm along a 10 km segment of the San Andreas fault near Station 2. The dislocation began at a point northwest of the recording site and propagated past and to the southeast of Station 2. The dislocation rise time and the seismic moment for this earthquake are estimated as 0.9 sec and 1.8×10^{25}

dyne cm, respectively. Our estimates here, when compared with other seismological observations suggest that the dislocation associated with the Parkfield earthquake is not uniform over the whole fault length of up to 37 km but concentrated along the 10 km segment near the southeastern end of the fault.

- A linear ramp dislocation time function appears to be superior to an exponential ramp function for interpretation of earthquake strong-motion records.

SECTION VIII
REFERENCES

- Aki, Keiiti, 1968, Seismic Displacements Near A Fault ; J. Geophysical Research, 73, pp. 5359-5375.
- Brown, R. D., Jr., and J. G. Vedder, 1967, Surface Tectonic Fractures Along the San Andreas Fault, The Parkfield-Cholame California Earthquakes of June-August 1966 ; U.S. Geological Survey Professional Paper No. 1579.
- Canitez, N., and M. N. Toksoz, 1972, Static and Dynamic Study of Earthquake Source Mechanism: San Fernando Earthquake, J. Geophysical Research, 77, pp. 2583-2594.
- Filson, J., and T. V. McEvelly, 1967, Love Wave Spectra and the Mechanism of the 1966 Parkfield sequence; Bulletin of the Seismological Society of America, 57, pp. 1245-1257.
- Haskell, N., 1969, Elastic Displacements in the Near-Field of a Propagating Fault, Bulletin of the Seismological Society of America, 59, pp. 865-908.
- Trifunac, M. D., and D. E. Hudson, 1971, Analysis of the Pacoima Dam Accelerogram - San Fernando, California, Earthquake of 1971, Bulletin of the Seismological Society of America, 61, pp. 1393-1411.
- Tsai, Y. B., and K. Aki, 1969, Simultaneous Determination of the Seismic Moment and Attenuation of Seismic Surface Waves, Bulletin of the Seismological Society of America, 59, pp. 275-287.

Whitcomb, J. H., 1971, Fault-Plane Solutions of the February 9, 1971, San Fernando Earthquake and Some Aftershocks, Professional Paper 733, pp. 30-32, U. S. Geological Survey, Washington, D. C.